



Modulation of the vertical particles transfer efficiency in the Oxygen Minimum Zone off Peru

Marine Bretagnon^{1,2*}, Aurélien Paulmier¹, Véronique Garçon¹, Boris Dewitte^{1,3,4}, Séréna Illig^{1, 5}, Nathalie Leblond⁶, Laurent Coppola⁶, Fernando Campos^{7,8,9}, Frederico Velazco¹⁰, Christos Panagiotopoulos¹¹, Andreas Oschlies¹², J. Martin Hernandez-Ayon¹³, Helmut Maske¹⁴, Oscar Vergara¹, Ivonne Montes⁸, Philippe Martinez¹⁵, Edgardo Carrasco¹⁰, Jacques Grelet¹⁶, Olivier Desprez-De-Gesincourt¹⁷, Christophe Maes^{1,18}, Lionel Scouarnec¹⁷

10

¹LEGOS (UPS/CNRS/IRD/CNES), Toulouse, France.

²ACRI, Sophia-Antipolis, France.

³Centro de Estudios Avanzado en Zonas Áridas (CEAZA), Coquimbo, Chile.

⁴Departamento de Biología, Facultad de Ciencias del Mar, Universidad Católica del Norte, Coquimbo, Chile.

15 ⁵Department of Oceanography, MARE Institute, LMI ICEMASA, University of Cape Town, Cape Town, Rondebosh, South Africa

⁶OOV, Villefranche sur Mer, France.

⁷UNAC, Lima, Peru.

⁸IGP, Lima, Peru.

20 ⁹CICESE, Ensenada, Mexico

¹⁰IMARPE, Callao, Peru.

¹¹MIO/CNRS, Marseille, France.

¹²GEOMAR/SFB754, Kiel, Germany.

¹³UABC, Ensenada, Mexico.

25 ¹⁴CICESE, Ensenada, B.C. Mexico

¹⁵EPOC, Bordeaux, France.

¹⁶US IMAGO/IRD, Brest, France.

¹⁷INSU/CNRS, DT, Brest, France.

¹⁸LOPS, Brest, France.

30

Correspondence to: Marine Bretagnon (marine.bretagnon@legos.obs-mip.fr)

Author contributions: M.B., A.P. and V.G. performed the research; A.P. and V.G. designed research; M.B., A.P., V.G., B.D., S.I., F.C., J.M.H-A., O.V., I.M., and P.M. analyzed the data and provided complementary analysis; M.B. and N.L. analyzed the sediment trap samples; A.P., V.G., B.D., N.L., L.C., F.C., F.V., C.P., E.C., J.G., O.D., A.O., J.M.H-A., O.V., C.M., and L.S. contributed to the sediment trap sampling and analysis as well to the mooring design and implementation; and M.B., A.P., V.G., B.D., C.P., P.M., and A.O wrote the paper.

35

Abstract

The fate of the Organic Matter (OM) produced by marine life controls the major biogeochemical cycles of the Earth's system. The OM produced through photosynthesis is either preserved, exported towards sediments or degraded through remineralisation in the water column. The productive Eastern Boundary Upwelling Systems (EBUSs) associated with Oxygen Minimum Zones (OMZs) should foster OM preservation due to low O₂ conditions, but their intense and diverse microbial activity should enhance OM degradation. To investigate this contradiction, sediment traps were deployed near the oxycline and in the OMZ core on an instrumented moored line off Peru, providing high temporal resolution O₂ series characterizing two seasonal steady states at the upper trap: suboxic ([O₂] <25 μmol.kg⁻¹) and hypoxic/oxic (15<[O₂]<160 μmol.kg⁻¹) in austral summer and winter/spring, respectively. The OMZ vertical transfer efficiency of Particulate Organic Carbon (POC) between

45



traps (T_{eff}) fits into three main ranges (high, intermediate, low) suggesting that both predominant preservation (high $T_{\text{eff}} > 50\%$) and remineralisation (intermediate $T_{\text{eff}} 20 < 50\%$ or low $T_{\text{eff}} < 6\%$) configurations can occur. An efficient OMZ vertical transfer ($T_{\text{eff}} > 50\%$) has been reported in summer and winter associated with extreme limitation in O_2 concentrations or OM quantity for OM degradation. However, higher levels of O_2 or OM, or less refractory OM, at the oxycline, even in a co-limitation context, can decrease the OMZ transfer efficiency below 50%, especially in summer during intraseasonal wind-driven oxygenation events. In late winter and early spring, high oxygenation conditions together with high fluxes of sinking particles trigger a shutdown of the OMZ transfer ($T_{\text{eff}} < 6\%$). Transfer efficiency of chemical elements composing the majority of the flux (nitrogen, phosphorus, silica, calcium carbonate) follows the same trend than for carbon, with the lowest transfer late winter and early spring. In terms of particulate isotopes, vertical transfer of $\delta^{15}\text{N}$ suggests a complex behaviour of ^{15}N impoverishment or enrichment according to T_{eff} modulation. This OM fate sensitivity to O_2 fluctuations and particles concentration calls for further investigations on OM and O_2 -driven remineralisation processes and the consideration of intermittent OMZ behaviour on OM in past studies and climate projections.

Introduction

Eastern Boundary Upwelling Systems (EBUSs) are generally known to be highly productive (Chavez and Messié, 2009), associated with significant primary production (479 to $1,213 \text{ gC}\cdot\text{m}^{-2}\cdot\text{yr}^{-1}$) and elevated concentrations of chlorophyll *a* (1.5 to $4.3 \text{ mg}\cdot\text{m}^{-3}$). This is because prevailing equatorward alongshore coastal winds trigger dynamic upwelling of cold nutrient-rich waters from the subsurface to the well-lit surface layer. The associated intense biological surface activity produces a large amount of Organic Matter (OM), part of which will sink and be degraded by catabolic processes. Therefore, subsurface OM degradation contributes to the consumption of oxygen (O_2) and, in conjunction with poor ventilation of the water mass, leads to the formation of Oxygen Minimum Zones (OMZs), characterized in the global ocean by a suboxic layer between 100 and 1,000 m in depth (Paulmier and Ruiz-Pino, 2009). OM degradation *via* respiration or remineralisation may influence biological productivity (fixed nitrogen loss and production of the toxic H_2S gas), and climate both on short and long timescales (Buesseler et al., 2007; Law et al., 2012; Moffit et al., 2015; Chi Fru et al., 2016) *via* modulation of the air-sea exchange of climatically-important gases (e.g. CO_2 , N_2O and CH_4). Moreover, these impacts on climate and ecosystems may be significant when remineralisation stimulated by high surface productivity takes place in waters that feed the upwelling close to the ocean-atmosphere interface (Helmke et al., 2005; Paulmier et al., 2008). Although poorly documented, the OM fate in OMZ stands out as a major issue, due to O_2 deficiency and its effect on remineralisation processes. Progress will depend on two different hypothesized mechanisms. On one hand, weak oxygenation appears to decrease OM degradation because anaerobic remineralisation is considered an order of magnitude less efficient than aerobic remineralisation (Sun et al., 2002), suggesting a tendency toward OM preservation and enhanced sediment export. On the other hand, the intense and diverse microbial activity (Devol, 1978; Lipschlutz et al., 1990; Azam et al., 1994; Ramaiah et al., 1996; Lam et al., 2009; Stewart et al., 2012; Roullier et al., 2014) may induce efficient remineralisation and/or respiration, especially in the more oxygenated, warmer upper OMZ layer associated with the oxycline, leading to substantial OM recycling. Remineralisation, involving a relatively variable stoichiometry in the OMZ (Paulmier et al., 2009), depends on several factors. Besides its quantity, OM recycling relies on quality (e.g., lability) and its sinking time through the OMZ layer. The relative depth of OM production compared to the depth of oxycline and O_2 availability is of particular importance, together with particle size and shape (Paulmier et al., 2006; Stemmann et al., 2004). The EBUS off Peru is one of the most productive systems, accounting for 10% of all world fisheries (Pennington et al., 2006; Chavez et al., 2008), with the shallowest oxycline and one of the most intense OMZs (Fig. 1a-b; Paulmier et al., 2009), so it provides perfect conditions to investigate the relative importance of the aforementioned mechanisms. In order to examine the particle



fluxes and their variability, this study focuses on the analysis of a time series compiled from moored sediment traps deployed in the Peruvian OMZ (Fig. 1c), as part of the AMOP (“Activities of research dedicated to the Minimum of Oxygen in the eastern Pacific”, see Methods) project.

Methods

5 A fixed mooring line has been deployed in January 2013 with R/V Meteor at ~50 km off Lima at 12°02'S; 77°40'W (Fig. 1) and recovered in February 2014 with R/V L'Atalante in the framework of the AMOP project (“Activities of research dedicated to the Minimum of Oxygen in the eastern Pacific”; <http://www.legos.obs-mip.fr/recherches/projets-en-cours/amop>). Along this line, sediment traps (PPS3 from Technicap Company) were deployed in the oxycline/upper OMZ core (34 m) and in the lower OMZ core (149 m) to study particle flux through the water column (Fig. 1c, Fig. 2 & S1; Tab. 1 & S1). The line was also equipped with five sensors measuring pressure, temperature, salinity and oxygen (SMP 37-SBE63), one sensor for fluorescence (ECO FLSB), and four additional temperature sensors (SBE56; Fig 1c). The oxygen sensors have a resolution (the smallest change detection) of 0.2 $\mu\text{mol.kg}^{-1}$, and an initial accuracy and detection limit of 3 $\mu\text{mol.kg}^{-1}$ (Fig. 3, Tab. 2). The resolutions and initial accuracies for the pressure, temperature, salinity sensors (0.2-0.7 and 0.1-0.35 dbar; 0.002 and 0.0001°C; 0.0003 and 0.00001; respectively) induce an estimated resolution and accuracy for density (Fig. 4a-b) of both 0.01 kg.m^{-3} according to the standard TEOS-10 equation. Each sediment trap was equipped with an inclinometer, which allows recording any potential inclination, fundamental for data interpretation. Also, to avoid organic matter decay (e.g. grazing) before analysis, OM was collected in a poisoned solution of sea water with 5% of formaldehyde. Traps sampled particles simultaneously over a period of seven days, during the three months of austral summer (AMOP1 period: January 06 to March 31, 2013). The mooring was serviced in June 2013. The mooring has been re-deployed on June 26, 2013 and collection of material in traps resumed on June 28. The sampling interval was extended to eleven days to fit the planned date of recovery and to cover a wider period including two seasons (austral winter-spring during AMOP2). The traps were full on November 06, 2013 but the mooring could not be recovered before February 2014 with R/V L'Atalante. Note that the SMP 37-SBE63 sensors started recording on January 5 at 34 m, on January 7 at 76 m, and on January 8 at both 147 and 160 m (Fig. 3), and on June 27, 2013 at 50 m only (due to a technical breakdown).

25 Before analyzing particle samples, we removed the swimmers, which could have actively entered the trap, and thus would not represent the strict vertical sinking mass flux. After freezing-drying, the mass flux (dry weight; Fig. S1, Tab. S1) was determined with an accuracy of $\pm 3\%$. Total carbon (C_{tot}), particulate organic and isotopic carbon (POC, $\delta^{13}\text{C}$) and nitrogen (PON, $\delta^{15}\text{N}$) were analyzed *via* an Isotope Resolved Mass Spectrometer (IRMS) Isoprime 100 paired with an Elementary Analyzer (EA) ElementarVarioPyrocube. The content of carbon and nitrogen (Fig. 2 & S2, Tab. 3a, S2a-b & S3) was measured with an accuracy of $\pm 0.2\%$, and the isotopic $\delta^{13}\text{C}$ and $\delta^{15}\text{N}$ measurements (Tab. 3c & S4) with an accuracy of $\pm 0.006\%$, and of 0.007 ‰, respectively. Phosphorus and silica (Tab. 3a & S2c-d-S3) were measured by a colorimetric method, using a spectrophotometer SPECOR 250 plus. Particulate Organic Phosphorus (POP), analyzed according to the classical method (Strickland & Parsons, 1972), was measured with an accuracy of $\pm 3\%$. The biogenic silica (BSi) was extracted with an alkaline dissolution at 95°C by a kinetic method (DeMaster, 1981) with an accuracy of $\pm 5\%$. Ca (for CaCO₃ estimation; Tab. S5) was determined from ICP-OES analysis with an accuracy of $\pm 3\%$. Systematic replicates for all sediment trap parameters have been analyzed to estimate a reproducibility, which mainly represents the sample heterogeneity. The reproducibility estimated from the Standard Deviation (SD) of the replicates for the total mass fluxes determination (0.12%) is generally lower than the accuracy, except for $\delta^{13}\text{C}$. In addition, daily satellite ASCAT wind (Fig. 4c-d), produced by Remote Sensing Systems (www.remss.com; sponsored by the NASA Ocean Vector Winds Science Team), has been used with an accuracy of 2 m.s^{-1} . The satellite wind data



are in agreement with the available *in situ* wind measured from the R/V METEOR during the initial mooring deployment, and wind direction corresponds to alongshore winds favorable to upwelling Ekman transport. The Mixed Layer Depth (MLD; Fig. 4c-d) has been estimated from a difference of temperature of 0.5°C following De Boyer Montegut et al. (2004), in phase with the 0.2°C and 0.8°C criteria. Finally, *in situ* pH_{sw} (Fig. S3) and calcite saturation state (Ω_{calcite}) were calculated with the CO2SYS program (Lewis and Wallace; 1998), using discrete Dissolved Inorganic Carbon measured using a LiCOR 7000 and potentiometric pH_{sw} measurements (25°C). The dissociation constants proposed by Lueker et al. (2002) were used for this purpose. This resulted in a precision of ± 0.04 units for pH_{sw} *in situ* and ± 0.2 units for Ω_{calcite} . Certified reference material (CRM) from Dr. Andrew Dickson's laboratory at Scripps Institution of Oceanography (University of California, San Diego) was used for assessing the precision and accuracy of measurements. The reference material gave a relative difference averaging 2.2 ± 1.1 $\mu\text{mol}\cdot\text{kg}^{-1}$, with a peak of $4 \mu\text{mol}\cdot\text{kg}^{-1}$ (0.2% error) with respect to the certified value.

The analysis accuracy for the sediment trap samples has been directly indicated in Fig. 2, and estimated by propagation of the accuracy of each parameter from a logarithmic expansion for the molar ratios (C:P, N:P, N:P, Si:C, Si:N and Si:P) and all the calculated vertical transfer efficiencies as T_{eff} for POC fluxes (cf. Eq. 1). Standard deviation (SD) between samples representing the variability over the total dataset (AMOP1+AMOP2) or a given subset of data (e.g. corresponding to high, intermediate or low T_{eff} ranges) has also been indicated in Tables 1, 2, 3 and S1, S2, S3, S4 and S5). The different relative SD present values always higher than the Total Uncertainties (TU = accuracy + reproducibility) for all considered parameters. Data are available at different time resolutions: 15 min (O_2 , density from temperature and salinity); 30 min (fluorescence); 1 day (satellite ASCAT wind); 7 or 11 days for AMOP1 and AMOP2 datasets, respectively (sediment trap fluxes, including the percentage of Polychaetes relatively to all other collected swimmers, noted %Poly). All fluxes (for the total mass of particles, POC, PON, POP, BSi, CaCO_3 , $\delta^{13}\text{C}$ and $\delta^{15}\text{N}$, as well as %Poly), corresponding to a period of collection of 7 and 11 days for AMOP1 and AMOP2 periods, respectively, have been normalized and expressed per day. Hereafter, we will use 7days as the nominal weekly period. Different averages have been performed to compare with different temporal resolution of other data: from 15 minutes resolution for O_2 , density and MLD and from 30 min resolution for the fluorescence to 1 day resolution (Fig. 4); from 15 minutes to 7 (for AMOP1) or 11 (for AMOP2) days resolution for O_2 (Tab. 2). We were cautious that different ways to average do not modify the main interpretations of the study. Note however that daily-average MLD (Fig 4c-d) presents a magnitude ~ 9 times smaller than with the 15min-frequency MLD, mainly due to biases induced by the vertical resolution according to the mooring sensors depths. For oxygen, the 1, 7 and 11 days averages have been noted $\overline{[\text{O}_2]}_{1\text{day}_{15\text{min}}}$, $\overline{[\text{O}_2]}_{7\text{days}_{15\text{min}}}$ and $\overline{[\text{O}_2]}_{11\text{days}_{15\text{min}}}$, respectively. $\overline{[\text{O}_2]}_{7\text{days}_{15\text{min}}}$ and $\overline{[\text{O}_2]}_{11\text{days}_{15\text{min}}}$ also allow defining the ratio of POC flux/ $[\text{O}_2]$, POC flux and $[\text{O}_2]$ being at the same temporal resolution (Tab. 2). This ratio corresponds to an availability index in terms of POC flux to be degraded according to the oxygen concentration availability. When this ratio POC Flux/ $[\text{O}_2]$ reaches extreme values far from the mean range (POC Flux/ $[\text{O}_2]$ > Average+SD or POC Flux/ $[\text{O}_2]$ < Average-SD), we define a severe limitation in oxygen only or in OM only, respectively, without co-limitation. When this ratio POC Flux/ $[\text{O}_2]$ is within the interval [average -SD, average +SD], we define a co-limitation with either O_2 or OM as the main factor limiting OM degradation.

Sediment trap fluxes, O_2 concentrations and other quantities considered in this study (e.g. the ratio of POC flux/ $[\text{O}_2]$) have been averaged on the different T_{eff} ranges (Tab. 1-3 & S1-S5).



RESULTS: Particles transfer efficiency through the OMZ

a) Temporal modulation of the particles and POC fluxes and of their transfer efficiencies

The transfer of particles through the Peruvian OMZ is studied using data collected at the two fixed sediment traps, one located in the oxycline/upper core (34 m) and the second in the lower core (149 m). Seasonally, at 34 m, the mass fluxes during summer are about 60% lower than during winter-spring (AMOP2: 986 mg.m⁻².d⁻¹ on average; cf. Fig. S1, Tab. S1). At 149 m, the mass fluxes during summer are about 80% higher than during winter-spring (AMOP2: 95 mg.m⁻².d⁻¹ on average; cf. Fig. S1, Tab. S1). Intra-seasonally, during summer (AMOP1), the variability of fluxes at 34 m and 149 m is 3 times and 40% lower than during winter-spring (AMOP2: SD = 144% (39<4647 mg.m⁻².d⁻¹) and 138% (12<488 mg.m⁻².d⁻¹), cf. Tab. S1), respectively. The POC flux (Tab. 1) is globally proportional to the total particle flux ($R^2 = 0.92$) (Fig. S2a). So that the analysis of the total particle flux or of the POC flux will lead to similar results. To investigate the influence of the oxygen deficient layer between both traps for each season, we use the POC transfer efficiency (T_{eff}) introduced by Buesseler et al. (2007), and defined as:

$$T_{\text{eff}} = \frac{POC_{149}}{POC_{34}} \times 100 \quad (1)$$

The transfer efficiency represents the ability of the system to preserve organic matter quantity and to foster the carbon export out of the productive layer. The higher is the transfer efficiency, the higher is the carbon export. A low T_{eff} suggests occurrence of remineralisation, which can recycle organic matter into available nutrients to sustain the high surface production.

T_{eff} values present a strong temporal variability and, while the mean transfer efficiency appears to be relatively similar for both datasets ($T_{\text{eff}} \sim 45\%$), the transfer appears to be more than 3 times more variable for AMOP2 than for AMOP1 (Fig. 2; Tab. 1). T_{eff} can be higher than 100%, meaning particles accumulation between both traps, potentially attributable to advection of particles or to primary or secondary production between traps. T_{eff} is never higher than 100% during AMOP1 but it is 3 times during AMOP2 (AMOP2-S1, -S3, -S6; $T_{\text{eff}} = 135, 106$ and 149% , respectively). Due to the potential bias affecting these values not linked to the influence of the OMZ, $T_{\text{eff}} > 100\%$ will be discarded. Except these very high T_{eff} , transfer efficiency varies between 1 and 71% and three ranges of variation can be defined: high, intermediate and low. The high range with a relatively efficient transfer ($T_{\text{eff}} > 50\%$) corresponds to a predominance of OM preservation. This preservation is observed for a third of the total samples, namely the first 3 samples of AMOP1 (AMOP1-S1, -S2 & -S3), the sample between 17 and 24 March (AMOP1-S11) and two samples in winter (AMOP2-S2 & -S5). Conversely, the other samples correspond to a predominance of OM degradation or remineralisation. The period occurring in late winter/early spring (from September 2 to November 6, representing half of the AMOP2 time period) seems to correspond to the period of main OM degradation, as the proportion of particles reaching the deeper trap is very low (low range of $T_{\text{eff}} < 6\%$). Between these extreme values, T_{eff} presents an intermediate range between 20 and 50%, occurring mainly in summer from January 27 to March 31 (AMOP1-S4, -S5, -S6, -S7, -S8, -S9, -S10 and -S12). Within the 20<50% T_{eff} range, the six samples in summer (AMOP1-S4, -S6, -S8, -S9, -S10 and -S12), and one sample in winter (AMOP2-S4) present a low intermediate T_{eff} range of 20<38%. The definition of these three main ranges of the transfer efficiency (low, intermediate, high) appears to be consistent since each one presents a slight variation with SD of 7% for $T_{\text{eff}} < 6\%$; of 7% for 20< T_{eff} <50%, and of 1% for $T_{\text{eff}} > 50\%$.

Note that the vertical profile of POC flux is assumed to follow a power law (Suess, 1980; Martin et al., 1987).

$$Flux_{149} = Flux_{34} * \left(\frac{149}{34}\right)^{-b} \quad (2)$$

The b coefficient represents the attenuation of the curve and therefore an index for OM respiration during its sinking. Fitting b on the AMOP dataset reveals temporally-varying b values (between 0.23. and 2.97, Tab. 1), with small and large b values, indicating a slow or rapid OM decay, respectively. Even if this transfer layer (between both traps) is relatively shallow and



covers a short distance (115 m) compared to other studies (e.g., between 200 and 1,000 m, Miquel et al., 2011; Heimbürger et al., 2013), b values are in the same range than previous estimates. The largest b values are estimated from September 2 (AMOP2-S7) to November 6 (AMOP2-S12) with a maximum of 2.97 on September 13 (AMOP2-S8). These high values correspond to the minimal transfer efficiency (low range of $T_{\text{eff}} < 6\%$) and are consistent with Martin's values observed for the oxygenated North Pacific (0.90 ± 0.06). The lower b values (between 0.23 and 0.98, Tab. 1) are in line with those generally observed in the Equatorial Pacific OMZ (between 0.63 and 0.9; Berelson, 2001), in the Peruvian OMZ (0.66 ± 0.24 ; Martin et al., 1987) and in the Arabian Sea OMZ (0.22 ; Roullier et al., 2014; 0.59 ± 0.24 ; Keil, 2016). The temporal modulation of b is comparable to the one associated with the spatial switch from the coast to the open ocean off Peru (Packard et al., 2015) as well as from high to low latitude configurations (Marsay et al., 2015). Globally, and in line with the transfer efficiency, the strongest attenuation is observed in spring ($b = 2.43 \pm 15\%$) while the weakest is recorded in winter ($b = 0.47 \pm 57\%$). One can notice that the attenuation is also 4 times stronger and 2.5 more variable in spring than in summer, where b is on average $0.62 \pm 39\%$. Considering ranges previously defined, $b = 2.43 (\pm 0.37)$ for low $T_{\text{eff}} (< 6\%)$, $b = 0.74 (\pm 0.15)$ for intermediate $T_{\text{eff}} (20 < 50\%)$ and $b = 0.36 (\pm 0.06)$ for high $T_{\text{eff}} (> 50\%)$.

b) Significance of the transfer efficiency

While the transfer efficiency (T_{eff}) between the upper (34 m) and lower (149 m) sediment traps allows a mathematical distinction between ranges of POC export efficiency, it is crucial to investigate the physical significance of this T_{eff} . Particles sampled at 149 m are not necessarily associated with the same vertical flux than those previously sampled at 34 m over the 7 or 11-days period due to the following three main processes: a) horizontal transport, b) vertical sinking speed defining the finite time between both traps and c) particle production between both traps involving different trophic levels.

T_{eff} may be affected by horizontal advection of particles and also by sediment trap line inclination, in response to the coastal current system (e.g., shear due to the northward flow at the surface and southward flow in the subsurface layers). These typical methodological biases in sediment trap studies are known to potentially affect the collection of particles and its efficiency. Here, the mean alongshore current (poleward) reaches $\sim 12 \text{ cm.s}^{-1}$ (slower than 15 cm.s^{-1}) over the duration of the experiment in vicinity of the sediment traps, according to *in situ* data (AMOP cruise), climatology (Chaigneau et al., 2013) and estimates from climatological regional model simulations (Montes et al., 2010; Dewitte et al., 2012). Therefore, the collection of particles is considered to be marginally affected by currents in this transfer layer (Baker et al., 1988), confirmed by a small inclination of the mooring line ($< 5^\circ$). However, the only three samples presenting values of $T_{\text{eff}} > 100\%$ (AMOP2-S1, -S3 and -S6) are characterized by a relatively high inclination anomaly (related to the mean inclination) of the mooring line, which can be assigned to a significant modification of the horizontal currents mean state. Zonal advection of particles from a more productive region in the lower trap could explain anomalous high transfer.

Vertically, we assume that upwelling or downwelling events (velocity below 0.5 m.d^{-1}) do not significantly impact particle sinking speed (ranging from 1 to $2,700 \text{ m.d}^{-1}$; Siegel et al., 1990; Waniek et al., 2000). In addition, the quantity of matter collected by the sediment trap in each cup at 149 m may be different to that collected in the corresponding cup at 34 m, depending on specific particles vertical velocities. Particle velocity also determines exposure time to a degradation activity in the water column. Therefore, the probability of particle degradation may increase for slower (generally smaller) particles spending a longer time in the subsurface active remineralisation layer between 34 and 149 m, which could be the case for samples with $T_{\text{eff}} < 50\%$. Conversely, the large amount of matter collected at 149 m for the high T_{eff} range ($> 50\%$) might be explained by potentially less-degraded particles, as a consequence of a faster sinking velocity (McDonnell et al., 2015). In theory, the sinking velocities of biogenic particles depend on various intrinsic factors (such as their sizes, shapes, densities, porosities) which can be modified along their fall by complex bio-physical processes (e.g. aggregation, ballasting, trimming by remineralisation), as well



as on the three-dimensional properties of the flow field (Stemmann and Boss, 2012). Note that particles aggregation (e.g. flocculation) or disaggregation should not modify the total mass flux but the quantity and the quality of the particles between both traps.

Finally, subsurface particles production between 34 and 149 m can affect T_{eff} , for instance when associated with a deep or
5 Secondary Chlorophyll Maximum (SCM), which can sometimes be more intense than the primary maximum in OMZ areas (Garcia-Robledo et al., 2017). The fluorometer data at 31 m suggest an intermittent increase in the fluorescence around this depth (Fig. 4e-f). However, the high fluorescence values could be attributable to the detection of an SCM or to deepening of the surface mixed layer, mixing the surface chlorophyll with the subsurface layer. To complement fluorescence data, $\delta^{13}\text{C}$ values (Tab. S4) provide some information about particle production and about typical processes linked to the surface productivity. Here, the
10 transfer efficiency of $\delta^{13}\text{C}$ is roughly constant (between 88% and 105%, Tab. S4), suggesting no significant primary production below the top trap and therefore no significant contribution of an SCM. In addition, since the water column between 34 m and 149 m is mostly below the euphotic layer where primary producers are mainly active, particles production is considered to be related to higher trophic levels only, in particular zooplankton (e.g. detritus due to excretion and mortality), which can also induce active vertical transport of particles not directly considered here. Zooplankton production should be pointed out for
15 AMOP1-S1, characterized by an oxygen event ($>10 \mu\text{mol.kg}^{-1}$, Fig. 4a), but with an unexpected high T_{eff} (71%) suggesting preferentially OM preservation. However, this sample is different from the others previously mentioned, with a number of swimmers collected 3 times higher than the average number for the AMOP1 dataset, especially in the lower trap and raising the influence of the active transfer between both traps and potentially secondary production.

In this study, we assume that a) similar particles are collected in the upper and lower traps for each sampling period; b)
20 all particles collected in the deep trap are, for each sampling period, subject to a comparable time in the OMZ layer. Note that all the AMOP1 samples in summer and the first six AMOP2 samples (from AMOP2-S1 to –S6) in winter appear to be subject to a comparable trophic level effect as samples are composed of around 60-70% of faecal pellets, spending therefore a homogeneous time in the OMZ. However, for the six last AMOP2 samples (from AMOP2-S7 to –S12) in late winter/early spring, the proportion of faecal pellets and marine snow inverts. For AMOP2 dataset, low T_{eff} (from AMOP2-S7 to –S12) can be explained
25 by the higher proportion of small particles (as marine snow) potentially easily degradable.

The transfer efficiency T_{eff} is controlled by the degradation of particles occurring below the productive layer. The organic matter degradation can be due to macro-organisms feeding (Lampitt et al., 1990) or to microbial activity (e.g. Devol, 1970; Lam et al., 2009; Stewart et al., 2012 and Roullier et al., 2014). These degradations imply a dependence on oxygen availability as it could constrain zooplankton in a specific layer, therefore limiting feeding, and it could reduce the microbial activity, as the aerobic
30 remineralisation is considered 10 times more efficient than anaerobic remineralisation (Sun et al., 2002). However, in addition to the catabolic energy's main requirement fuelled by O_2 availability, OM bio-availability should feed the substrate anabolic requirement of the heterotrophic microbial community controlling remineralisation activity. This is in line with previous studies showing microbial nitrogen cycling regulated by OM export (Kalvelage et al., 2013). Therefore, for intermediate ($20 < T_{\text{eff}} < 50\%$) and high T_{eff} ($>50\%$), OM degradation is considered as limited, whereas for low T_{eff} ($< 6\%$) it is not. The role of oxygenation and
35 OM availability on the OM degradation is explored to better estimate if the quantity of carbon still remains available for the surface production and air-sea exchange or if it is preserved and exported toward the sediment.



DISCUSSION

The respective roles of oxygen and organic matter in modulating the transfer efficiency will be evaluated.

a) The role of oxygen

5 The transfer efficiency (T_{eff}) presents variation between seasons, as well as at an intraseasonal scale. The role of oxygen is investigated by considering temporal changes in oxygenation as a potential factor associated with changes in remineralisation activity to explain the T_{eff} modulation.

Vertical and temporal $[O_2]$ changes mainly occur near the oxycline and upper OMZ core (upper trap) rather than in the lower OMZ (lower trap), where O_2 concentration remains stable, reaching the lowest detection limit (Fig. 3). Close to the upper trap, oxygen concentration can then be a key-factor triggering limitation of remineralisation.

10 Seasonally, mean oxygen concentration appears to be ~10 times lower for AMOP1 (~5 $\mu\text{mol.kg}^{-1}$) than for AMOP2 (~60 $\mu\text{mol.kg}^{-1}$; Fig. 4a-b). The daily-averaged oxygen concentration at 34 m points out the existence of two steady states in terms of oxygenation: i) the suboxic conditions occurring in summer, where $[O_2]$ stays below 25 $\mu\text{mol.kg}^{-1}$, and/or with a shallower oxycline; ii) the hypoxic/oxic conditions occurring in winter and early spring, where $[O_2]$ is always above 15 $\mu\text{mol.kg}^{-1}$, and/or with a deeper oxycline (Fig. 4a-b). Suboxia corresponds to limiting conditions for both aerobic micro- and macro-biological (e.g. bacteria and zooplankton) OM degradation thereby impacting the vertical transfer efficiency (T_{eff}). This is confirmed by swimmers abundance during AMOP1 twice as low than during AMOP2. This is also confirmed by the relative abundance of polychaetes, known to better tolerate suboxic conditions than copepods, which is 22 times higher at the oxycline during AMOP1 than during AMOP2 (Tab. 2). Oxygen concentration may also indirectly impact T_{eff} , since more oxygenated conditions (e.g. during AMOP2) allow micro-organisms such as copepods to colonize depths around the upper trap which can potentially produce particles between both traps through sloppy feeding, faecal pellets and carcasses sinking. The latter mechanism can also be suggested to explain the higher than 100% T_{eff} .

In addition to concentration considerations, $[O_2]$ for AMOP1 is 10 times less variable ($SD= 2.6 \mu\text{mol.kg}^{-1}$ for $\overline{[O_2]}_{7\text{days}_{15\text{min}}}$) than for AMOP2 ($SD=28 \mu\text{mol.kg}^{-1}$ for $\overline{[O_2]}_{11\text{days}_{15\text{min}}}$; Tab. 2). This difference in terms of variability highlights less intense and 2 times less frequent oxygenation events during AMOP1 than during AMOP2 (Fig. 4a-b). More elevated O_2 -conditions observed during AMOP2 are favourable to OM degradation through both micro- and macro-organisms, and are thus in agreement with a lower T_{eff} (<6%), where no-limitation of the degradation mechanisms is considered.

30 Intra-seasonally, for AMOP1 associated with an O_2 limitation period, specific relative and significant oxygenation conditions ($5.5 \leq 12.5 \mu\text{mol.kg}^{-1}$) can be identified according to the weekly averages. Those oxygenation conditions, 30% higher than the seasonal mean O_2 steady state, occur between: January 6 and 13 (AMOP1-S1); January 27 and February 3 (AMOP1-S4); February 10 and 17 (AMOP1-S6); February 24 and March 17 (AMOP1-S8, -S9, -S10; Tab. 2, Fig. 4a). In such cases, an aerobic remineralisation could be still active and potentially coupled with underlying anaerobe remineralisation leading to a relatively more efficient OM degradation (Sun et al., 2002), in agreement with relatively low T_{eff} ($24 \leq 38\%$; Tab. 1), except for AMOP1-S1 (considered apart; cf section *Significance of the transfer efficiency*). On the contrary, less oxygenated conditions ($3.5 \leq 4.9 \mu\text{mol.kg}^{-1}$) inducing potential O_2 limitation are in agreement with relatively higher intermediate T_{eff} ($38 \leq 57\%$ for AMOP1-S2, -S3, -S5, -S7, -S11, -S12). In these cases, a severe O_2 limitation can be considered, as the oxygen concentration appears to be about 25% lower than the seasonal mean O_2 steady state. This severe O_2 limitation also covered situations considered limited by



O₂ only (POC flux/[O₂] > Average+SD meaning >17+10: AMOP1-S2&3) but also by OM only (POC flux/[O₂] < Average-SD, meaning <17-10: AMOP1-S11).

At higher frequency, within the weekly period, the oxygenated conditions present oxygenation episodic events with: i) a higher daily occurrence (≥ 2 per week; up to 6 events for AMOP1-S8); ii) often relatively intense ($\overline{[O_2]}_{1day_{15min}}$ reaching 24.2 $\mu\text{mol.kg}^{-1}$ for AMOP1-S9; Fig. 4a). On the contrary, the less oxygenated conditions do not present or present very weak (≤ 2 per week) occurrence of oxygenation events, which are generally less intense.

The oxygenation events, reported for both AMOP1 and AMOP2, are linked with density minima ($< 26.1 \text{ kg.m}^{-3}$) and match relatively well a Mixed Layer Depth (MLD) deepening, suggesting vertical diapycnal mixing with surface water (Fig. 4a-b-c-d). Induced vertical mixing appears to be driven by increase in wind intensity, frequency (more than one wind pulse per week) and duration (~ 10 days). Globally, the averaged density for AMOP2 is lighter than AMOP1 by $\sim 0.07 \text{ kg.m}^{-3}$. Short wind-driven mixing events are followed by a longer re-stratification time period associated with an [O₂] decrease (of $\sim 5 \mu\text{mol.kg}^{-1}$ for AMOP1 and $> 20 \mu\text{mol.kg}^{-1}$ up to $100 \mu\text{mol.kg}^{-1}$ for AMOP2) and density increase (of $> 0.1 \text{ kg.m}^{-3}$, up to 0.4 kg.m^{-3} for AMOP 2), then stabilization. The sequences of mixing/stratification and oxygenation/deoxygenation could be induced by sequences of stirring (or downwelling)/upwelling. These sequences are typically observed during an upward transportation of deeper, denser and lower [O₂] water, in response to a modulation in alongshore winds favourable to Ekman transport. A propagation of coastal trapped waves, with in phase vertical fluctuations in the density and oxygen isopleths, can also take place (Sobarzo et al., 2007; Dewitte et al., 2011 and Illig et al., 2014). These wind-driven oxygenation events, in period of the lowest seasonal steady state oxygenation as during AMOP1, potentially modulate the intensity of remineralisation at an intra-monthly frequency. Actually, during summer (AMOP1), while transfer efficiency varies up to a factor of 2 (24<57%), oxygenation events, allowing less O₂ limitation, are in agreement with a relatively lower intermediate T_{eff} between 20% and 40% (e.g. for AMOP1-S4, -S6, -S8, -S9 and -S10).

The transfer efficiency (T_{eff}) decreases from high ($> 50\%$) to low intermediate (20<38%) when [O₂] at the oxycline, or in the upper OMZ, increases during oxygenation events: i) at seasonal scale from the limit of detection of $\overline{[O_2]}_{1day_{15min}}$ higher than $\sim 5 \mu\text{mol.kg}^{-1}$ up to $\sim 25 \mu\text{mol.kg}^{-1}$ in summer; ii) at intraseasonal scale from less ($\sim 5 \mu\text{mol.kg}^{-1}$ in summer) to more ($\sim 60 \mu\text{mol.kg}^{-1}$ in winter/spring) oxygenated mean states. However, for the similar winter/spring hypoxic/oxic conditions at the oxycline, the modulation of T_{eff} (between 1% and 68%) suggests that another factor than oxygen constrains the mechanism of OM degradation and remineralisation.

b) The role of Organic Matter

In addition to oxygen, as well as transport mechanisms, sinking time and trophic transfer considered as biases, other processes depending on particles nature may explain the contrasted transfer (T_{eff}). Collected particles are marine and organic and can be mainly considered as OM, in agreement with the similar modulation of T_{eff} for POC and the transfer efficiency for the total particles (Fig. S1, S2 and

S4). Indeed C:N ratios at 34 m (between 5.7 and 10.1, Tab. 3b and S3a) are always below 20, characteristic of a marine origin (Mayers, 1993), although approximately 13% higher than the canonical Redfield values (Redfield et al., 1963). Carbon isotopic signatures ($\delta^{13}\text{C}$) are between -22.7 and -17.4‰ and $\delta^{15}\text{N}$ between 3.5 and 13.1‰ (Tab. 3c and S4), consistent with marine organic compounds, and inconsistent with a specific terrigenous influence (Degens et al., 1968; Ohkouchi et al., 2015; Bardhan et al., 2015).



Variability in the exported OM acts as anabolic biogeochemical forcing, supplying the OMZ with particles to be degraded and remineralised, and thereby potentially mitigating the transfer efficiency (T_{eff}). The variability of the particles flux collected in the upper trap is thus considered to understand the role of OM quantity and quality on the transfer efficiency (T_{eff}).

Quantitatively, the POC flux at 34 m presents a seasonal variability, with values 40% higher during AMOP2 than AMOP1 (on average 131 and 93 $\text{mgC}\cdot\text{m}^{-2}\cdot\text{d}^{-1}$, respectively), and with a stronger variability (AMOP2 being more than 1.5 times more variable). This is confirmed with the fluorescence measurement at 31 m, higher for AMOP2 than for AMOP1 (Fig. 4e-f). Actually, a deepening of the MLD as a response to the wind strengthening can increase the fluorescence values at 31 m by stronger vertical mixing with chlorophyll produced at surface. Thus, mixing of the surface productivity with the subsurface layers could contribute to an increase of the fluorescence in subsurface.

During the AMOP2 winter period, in hypoxic/oxic conditions, low light availability and high mixing (Fig. 4d) induce a low surface productivity according to lower fluorescence values at 31 m, contributing to the low POC flux recorded by the upper trap (Fig. 4f). Conversely in spring, while the water column is stratifying (MLD decrease; Fig. 4d), the surface productivity increases in agreement with higher fluorescence values (globally higher than $1\mu\text{g}\cdot\text{l}^{-1}$), leading to a higher concentration of particles and to a POC flux about 10 times stronger than in winter ($239.58 > 24.79\text{ mgC}\cdot\text{m}^{-2}\cdot\text{d}^{-1}$; Fig. 2b&4f). The T_{eff} decrease from winter to early spring, characterised by high and intermediate ($>20\%$) and low ($<6\%$) values, respectively, follows a power tendency line (Fig. 5).

During AMOP1 in suboxic conditions at the oxycline and O_2 limitation of OM degradation, the events of slight oxygenation have supported the modulation of T_{eff} from high ($>40\%$; AMOP1-S2, -S3, -S5, -S7, -S11) to low ($<40\%$; AMOP1-S6, -S8, -S9, -S10) intermediate values, except for AMOP1-S1 (considered apart; cf. section *Significance of the transfer efficiency*). Now, considering the variability of OM quantity together with O_2 availability allows analysing the differences of the transfer efficiency (T_{eff} below or above 50%) characterizing OMZ remineralization-like and preservation-like configurations, respectively. The highest POC fluxes ($>85\text{ mgC}\cdot\text{m}^{-2}\cdot\text{d}^{-1}$) at 34 m occur from AMOP1-S1 to -S6 and AMOP1-S8 to -S9, whereas for AMOP1-S7 and from AMOP1-S10 to -S12, POC fluxes are $\sim 30\%$ lower than the seasonal average (Fig. 2a&4e). The low OM quantity could therefore explain a weaker remineralisation, and thus a slightly higher T_{eff} (up to 57%). However, limitation of both O_2 and OM, simultaneously (co-limitation) or not, should be considered. When the ratio POC Flux/ $[\text{O}_2]$ is far from the mean range and defines a severe limitation in OM only (<7 for AMOP1-S11) or O_2 only (>27 for AMOP1-S2&3), T_{eff} becomes high. Conversely, when the ratio POC Flux/ $[\text{O}_2]$ remains closer to the mean range ($7 < 27$) for AMOP1-S4, -S5, -S6, -S7, -S8, -S9, -S10 & -S12, except for AMOP1-S1 (considered apart; cf. section *Significance of the transfer efficiency*), T_{eff} remains intermediate ($20 < 50\%$) associated with a potentially balanced co-limitation in O_2 and OM on OM degradation.

Qualitatively, the evolution of elemental fluxes at 34 m should be taken into account to investigate whether the composition of a more or less labile OM can affect the transfer efficiency (T_{eff}) in addition to the OM availability. For both datasets, POC and PON fluxes show a strong linear correlation with the total particles mass fluxes at the upper trap as well as for the lower trap ($R^2 = 0.98$ for both traps Fig. S2a, b).

In order to study the influence of the particles quality on the transfer efficiency, the composition is averaged for the three main ranges of T_{eff} . Also, as the matter collected in the trap is mainly organic, only the four main components (POC, PON, POP and BSi) were considered here. Whatever the range of T_{eff} , the particles flux is dominated by POC, then BSi, PON and POP contribute in different proportions (Fig. 6b; Tab. 3a&S2). For low T_{eff} , POC dominates with only 49%, whereas for intermediate including AMOP2-S4 and high T_{eff} ranges, POC remains relatively constant reaching 65-66% of the total POC+BSi+PON+POP.



On the contrary, BSi reaches 43% for low T_{eff} , whereas for the relatively constant intermediate and high T_{eff} ranges, BSi is reaching 25% only. Whatever the T_{eff} range, PON and POP have a relatively stable contribution of 7-8% and 1-2%, respectively. Between intermediate and high T_{eff} ranges, the relative constancy in the composition of the particles does not allow the investigation of the influence of the quality on the transfer efficiency.

5 Nevertheless, for the remineralisation event observed on AMOP2-S4, while OM quantity was expected to limit remineralisation, the influence of the quality should be pointed out as another factor acting on its low intermediate T_{eff} (32%; Fig. 6, Tab. 1). Indeed, this sample is specifically characterized by a relatively low BSi content (~ 19%, 50% lower than the winter average) and the highest PON and POP proportions (35% and 5 times higher than the winter average, respectively, Fig. 6b; Tab. S2). For this sample, the relative proportion of BSi decreases and the one of PON increases as compared to the other intermediate, low and
10 high T_{eff} samples, leading to less refractory and more labile matter, preferentially degraded. The difference in composition for this sample could also be noticed in terms of calcium carbonate which exhibits a maximum at this date compared to other intermediate and high T_{eff} (Tab. 3c) and about 5 times higher (20% of the total mass flux) than the average for the entire dataset (Tab. S5). A difference of phytoplankton community could be at the origin of this distinction. Indeed, at the beginning of the AMOP2 dataset and up to this sample, the MLD is relatively stable and no strong deepening is observed as a consequence of
15 wind intensification. As the surface productivity is mainly due to diatoms, this long period without strong mixing event can induce silica depletion in surface, limiting diatoms growth. This hypothesis is supported by the analysis of the phytoplankton functional types around the mooring location using MODIS data and the algorithm developed by Hirata et al. (2011). For AMOP2-S4, the prymnesiophyceae becomes the most influent phytoplanktonic group. The dominance for this sample of the prymnesiophyceae can induce a change in the composition of the sinking particles, in particular decreasing their BSi proportion,
20 leading to a more labile matter.

The composition of the matter at the upper trap can also be observed as a function of the particulate molar ratios to identify the relative elemental excess or deficit. Whatever the considered range of T_{eff} , biogenic silica appears to be in excess as Si:C, Si:N and Si:P are in average 3.9, 4.4 and 3.0 times higher than the classical ones, respectively (Tab. S3b). The strongest BSi excess can be assessed for low T_{eff} (ratio ~5 times higher than the classical ones; Tab. 3b). For the other elemental ratios, one can notice
25 that low T_{eff} appears to be different than the other T_{eff} ranges. Indeed, low T_{eff} presents a relative POP deficit (C:P and N:P ~20% higher than classical ones) with a C:N ratio equal to classical one (6.67). On the contrary, the other T_{eff} ranges present a relative POP excess (C:P and N:P about twice as low than classical ones), with a PON deficit relatively to POC (C:N) between 12 and 24%.

Molar ratios at 34 m for AMOP2-S4 are confirming the analysis of the elemental composition (Fig. 6b), especially BSi deficit
30 (e.g. Si:C and Si:N about twice as low and Si:P ~4 times lower than classical ones) and P excess (C:P and N:P ~8 times higher than classical ones; Tab. S3). However, Si:P, C:N, C:P and N:P present a strong variability (relative SD reaching 60% for the intermediate T_{eff} range), and especially with values below or above the classical reference ones, whatever the T_{eff} range.

Therefore, the OM quantity produced above the oxycline appears to have a stronger influence on the transfer efficiency than the OM quality of the sinking particles, although more or less labile materials can also contribute to better preserve and
35 export particles towards sediment or remineralise them in the upper layers of the ocean. Together with oxygenation conditions, OM quantity appears as a main factor triggering strong remineralisation, which could be strengthened or mitigated by OM quality considered here as a secondary factor.



c) Comparisons of transfer efficiencies for POC and other particles components

The analysis of the particles transfer efficiency through the OMZ has been focussed on carbon element, defining three main T_{eff} ranges. Here, the transfer efficiencies of other particles components (T_{effPON} for PON, T_{effPOP} for POP, T_{effBSi} for BSi, T_{effCaCO_3} for CaCO_3 , $T_{\text{eff}^{13}\text{C}}$ and $T_{\text{eff}^{15}\text{N}}$ for isotopic signatures) as well as their modulation and distribution, are studied.

5 All transfer efficiencies for the elemental composition present a low range (<15%) clearly dissociated from intermediate (15<55%) and high (55<80%) ranges, even if T_{effPOP} shows a more gradual transition between 0 and 55% (Tab. S2). Due to the similar distribution of the transfer efficiency ranges for POC and for other elemental components, the three main T_{eff} ranges (low, intermediate, high) defined for T_{eff} are kept (Fig. 7; Tab. 3). However at low T_{eff} , T_{effPOP} remains much higher than 6% (15%), corresponding to a decrease from the intermediate range five times lower than for the other elements. This indicates a
 10 relative accumulation of phosphorus, suggesting that in remineralisation-like configuration, phosphorus material remains more refractory than for the other components, such as the more labile nitrogen-rich amino-acids material preferentially degraded (Van Mooy et al., 2002; Böning et al., 2004; Pantoja et al., 2004; Diaz et al., 2008). In the preservation-like configurations (high T_{eff}), T_{effCaCO_3} becomes higher than 100% (133%), suggesting a potential accumulation and/or aggregation of calcium carbonate particles (e.g. from coccolithophorids or planktonic foraminifera) with depth. Indeed, for high T_{eff} range, the CaCO_3 flux
 15 collected in the deep trap appears to be about twice as high as the global average (Tab. 3c&S5), indicating a higher density of particles between both traps which can therefore aggregate. The comparison from high to intermediate T_{eff} ranges shows a T_{effCaCO_3} decrease twice as high as for the other components (T_{eff} , T_{effPON} , T_{effPOP} and T_{effBSi}). T_{effCaCO_3} decrease for CaCO_3 , known for its refractory properties, could be associated with a stimulation of significant water column dissolution (e.g. Orr et al., 2005). Since intermediate T_{eff} range corresponds to a large predominance at ~90% of summer AMOP1 (Tab. 1), the explanation is
 20 focused on AMOP1 only and based on the following consideration: the water column between the upper and lower traps is highly oxygen depleted, and theoretically, the lowest O_2 concentrations correspond to the lowest pH values (<7.5 SWS), since the OMZ is associated not only with high microbial activity but also with an acidified layer. Actually according to AMOP cruise cross-shore sections, local O_2 fluctuations are associated with pH fluctuations, especially in intensity and depth near the oxycline (7.4<8.4 SWS, Fig S3) and the calcite horizon ($\Omega_{\text{calcite}} \sim 1$; Paulmier and Ruiz-Pino, 2009; Paulmier et al., 2011; Leon et al.,
 25 2011). However the high T_{eff} for CaCO_3 may be driven by AMOP2 samples. Indeed, high oxygen concentrations during AMOP2 may lead to high pH conditions and therefore to CaCO_3 preservation. As this element is more refractory, it could accumulate along the water column, and explain the high transfer efficiency.

The study of the vertical transfer efficiency of the elemental ratios ($T_{\text{effC:N}}$ for C:N, $T_{\text{effC:P}}$ for C:P, $T_{\text{effN:P}}$ for N:P, $T_{\text{effSi:C}}$ for Si:C, $T_{\text{effSi:N}}$ for Si:N and $T_{\text{effSi:P}}$ for Si:P; Tab. 3b&S3) is confirming the previous analysis (from Fig. 7). The vertical transfer
 30 efficiency $T_{\text{effC:N}}$ remains relatively constant from low to high T_{eff} ranges, in agreement with the co-variation of POC and PON fluxes at the upper and lower traps and of T_{eff} and T_{effPON} (Fig. S2b & d). During the remineralisation-like configuration, the vertical C:P and N:P transfer efficiencies sharply decrease by a factor 3 from intermediate to low $T_{\text{effC:P}}$ and $T_{\text{effN:P}}$ reaching ~35% (Tab. 3b), which confirms the relative enrichment of the more refractory phosphorous materials. Also, C:P and N:P ratios, higher than classical ones in the upper trap, become lower than classical values in the lower trap. The transfer efficiency of the
 35 molar ratios involving BSi, with relatively constant Si:C and Si:N and a huge decrease by a factor 7 for Si:P from high to low T_{eff} ranges, is more complex to analyze. The antagonist interplay of the refractory BSi properties and the low pH dissolution on BSi (e.g. Loucaides et al., 2008) has to be considered, in addition to recycling mainly occurring at the sediment/water interface (e.g. Tréguer and De La Rocha, 2013).

In line with paleoceanographic studies, it should be interesting to focus on evolution of particulate $\delta^{13}\text{C}$ and $\delta^{15}\text{N}$ as a
 40 function of the T_{eff} ranges. $T_{\text{eff}^{13}\text{C}}$ and $T_{\text{eff}^{15}\text{N}}$ remain around 100% whatever the T_{eff} ranges (Fig. 7, Tab. 3c). While $\delta^{13}\text{C}$ appears



to slightly decrease during particles sinking (average $T_{\text{eff}3\text{C}}$ of 95%; Tab. S4), no significant $T_{\text{eff}3\text{C}}$ distinction between low, intermediate and high T_{eff} ranges could be done. For all T_{eff} ranges and all considered seasons, carbon isotope appears to be slightly heavier in the lower trap (Tab. S4), potentially indicating a greater influence of inorganic carbon with depth. The $T_{\text{eff}5\text{N}}$ variation appears to be stronger than $T_{\text{eff}3\text{C}}$, varying between 83 and 267% (average of $125\% \pm 37\%$). $T_{\text{eff}5\text{N}}$ remains higher than 100% for all main T_{eff} ranges, in agreement with a particulate $\delta^{15}\text{N}$ decrease with depth from the oxycline to the OMZ core in response to remineralisation mechanisms reported previously off Peru (Libes and Deuser, 1988). Thus, in addition to the particulate $\delta^{15}\text{N}$ alteration due to the microbial activities and the chemical and isotopic PON compositions associated with different metabolic pathways of OM synthesis, the depth and oxygenation of the oxycline should play an important role to explain the differences between low, intermediate and high T_{eff} ranges. Actually, the highest $T_{\text{eff}5\text{N}}$ (156%) occurs for the intermediate T_{eff} range, whereas $T_{\text{eff}5\text{N}}$ are lower (107 and 113%) for the low and high T_{eff} ranges, respectively. However one should be cautious with these results, as the variability in $\delta^{15}\text{N}$ on the entire dataset does not allow to strictly discriminate the ranges.

Therefore, in the OMZ, short-term $[\text{O}_2]$ fluctuations and particles loading appear to be important and should be considered for further studies on OM fate, carbon sequestration, nutrient regeneration, and greenhouse and toxic dissolved gas production or consumption. These impacts call for the development of variable molar ratio models for OM production mechanisms, but also OMZ remineralisation processes, and for the revised interpretation of paleoproxies.

Summary and conclusion

The seasonal and intraseasonal analysis of particles, collected using sediment traps in the oxycline and the core of the Peruvian EBUS, confirms that the OMZ can behave either as a recycling or a preservation system for Organic Matter (OM). Transfer efficiency (T_{eff}) presents variations which can be classified in three main characteristic ranges (high with $50 < T_{\text{eff}} < 75\%$ associated with preservation capacity, intermediate with $20 < T_{\text{eff}} < 50\%$ and low with $T_{\text{eff}} < 6\%$, associated with remineralization capacity), representing a more or less efficient carbon export through the OMZ. Seasonally, two different steady states are defined for oxygen conditions. The suboxic regime ($[\text{O}_2] < 25 \mu\text{mol.kg}^{-1}$) occurs mainly in austral summer, and the hypoxic/oxic regime in austral winter and early-spring ($15 < [\text{O}_2] < 160 \mu\text{mol.kg}^{-1}$). While suboxia is expected to foster OM preservation and therefore enhance the transfer efficiency, low O_2 conditions occurring in austral summer can also induce weak remineralisation, consequently to intra-seasonal wind-driven oxygenation events. In addition to oxygenation conditions, sinking particles from the oxycline play a role on the transfer efficiency. Indeed, the high POC flux ($> 80 \text{ mgC.m}^{-2}.\text{d}^{-1}$) end of winter/early spring can provide enough substrates to sustain the anabolic requirement of the microbial activity, and shut down the vertical transfer ($T_{\text{eff}} < 6\%$). On the contrary, the extreme deficits in oxygen ($[\text{O}_2] < 5 \mu\text{mol.kg}^{-1}$ at the oxycline) or in OM ($< 40 \text{ mgC.m}^{-2}.\text{d}^{-1}$) lead to the most efficient POC transfer ($T_{\text{eff}} > 50\%$) for both summer and winter seasons, considered as a limitation for OM degradation activity (e.g. microbial remineralisation and zooplankton feeding on particles). Between high and low T_{eff} , higher levels of O_2 or OM, even in a co-limitation context, can lead to an OMZ transfer efficiency slightly decreased ($20 < 50\%$), especially in summer ($20 < 40\%$). Since the composition of particles documented in the Peruvian OMZ could be considered as stable, mainly composed of POC and BSi, OM quality does not appear to be the main factor leading to T_{eff} modulation. But punctually, the occurrence of nitrogen-rich organic compounds in relatively well oxygenated water could strengthen a remineralisation activity, with low intermediate T_{eff} (32%). This study reconciles two opposite views concerning the OMZ behaviour on OM cycling, supporting the existence of both dynamic and static balanced biogeochemical states defined as states with and without significant remineralisation and O_2 consumption, respectively. The key microbial feedback on particles



including their elemental composition should be further investigated along with detailing the role of OM quality. This is expected to lead to a better understanding of the vertical OM transfer efficiency of the OMZ and its modulation. Climate projections and paleoceanography studies should therefore take into account the intermittence of the OMZ preservation or recycling capacity, crucial for global biogeochemical budgets.

5

Acknowledgements

We would like to thank the crew of the German R/V Meteor for the deployment as part of the DFG-funded SFB754 fieldwork, the crew of the Peruvian R/V Olaya for the visit and the crew of the French R/V Atalante for the recovery of the fixed AMOP mooring. We would like to thank Stefan Sommer and Marcus Dengler for providing the METEOR wind dataset. We would also like to thank Miriam Soto, Anne Royer and Emmanuel De Saint Léger for general logistics and administrative support. We are grateful to Vincent Rossi for discussions regarding the processes affecting the sinking speed of the particles. We are finally also grateful to Christophe Lerebourg, from ACRI-ST for his support during the course of this study. This work was supported by the AMOP (“Activity of research dedicated to the Minimum of Oxygen in the eastern Pacific”) project supported by IRD, CNRS/INSU, DT-INSU and LEGOS, and by a GIS COOC (UPMC, INSU/CNRS, CNES, ACRI-ST) Ph.D. grant.

15

Literature cited

Azam, F., Steward, G. F., Smith, D. C. and Ducklow, H. W.: Significance of bacteria in carbon fluxes in the Arabian Sea, *Earth Planet. Sci.*, 103(2), 341-351, 1994.

Baker, E. T., Milburn, H. B. and Tennant, D. A.: Field assessment of sediment trap efficiency under varying flow conditions, *J. Mar. Res.*, 46(3), 573-592, 1988.

Bardhan, P., Karapurkar, S. G., Shenoy, D. M., Kurian, S., Sarkar, A., Maya M. V., Naik, H., Varik, S. and Naqvi, S. W. A.: Carbon and nitrogen isotopic composition of suspended particulate organic matter in Zuari Estuary, west coast of India, *J. Mar. Syst.*, 141, 90-97, 2015.

Berelson W. M.: The flux of particulate organic carbon into the ocean interior: A comparison of four U.S. JGOFS regional studies, *Oceanography.*, 14(4), 59-67, 2001.

Böning, P., Brumsack, H. J., Böttcher, M. E., Schnetger, B., Kriete, C., Kallmeyer, J. and Borchers, S. L.: Geochemistry of Peruvian near-surface sediments, *Geochimica and Cosmochimica Acta.*, 68(21), 4429-4451 2004.

Brzezinski, M. A.: The Si: C: N ratio of marine diatoms: interspecific variability and the effect of some environmental variables, *Journal of Phycology*, 21(3), 347-357, 1985.

Buesseler, K. O., Lamborg, C. H., Boyd P. W., Lam, P. J., Trull, T. W., Bidigare, R. R., Bishop, J. K. B., Casciotti, K. L., Dehairs, F., Elskens, M., Honda, M., Karl, D. M., Siegel, D. A., Silver, M. W., Steinberg, D. K., Valdes, J., Van Mooy, B. and Wilson S.: Revisiting carbon flux through the ocean's twilight zone, *Science*, 316, 567-570, 2007.

30



- Chaigneau, A., Domingez, N., Eldin, G., Flores, R., Grados, C. and Echevin, V.: Near-Coastal circulation in the Northern Humboldt Current System from shipboard ADCP data, *J. Geophys. Res.*, 118(10), 5251-5266, 2013.
- Chavez, F. P. and Messié, M.: A comparison of Eastern Boundary Upwelling Ecosystems, *Prog. Oceanogr.*, 83, 80-96, 2009.
- Chavez, F. P., Bertrand, A., Guevara-Carrasco, R. and Csirke, J.; The northern Humboldt Current System: Brief history, present status and a view towards the future, *Prog Oceanogr.*, 79, 95-105, 2008.
- Chi Fru, E., Rodriguez, N.P., Partin, C. A., Lalonde, S. V., Andersson, P., Weis, D. J., El Albani A., Rodushkin, I. and Konhauser, K. O.: Cu isotopes in marine black shales record the Great Oxidation Event, *Proc Natl Acad Sci USA.*, 113(18), 4941-4946, 2016.
- de Boyer Montegut, C., Fischer, A. S., Lazar, A. and Iudicone, D.: Mixed layer depth over the global ocean: An examination of profile data and a profile-based climatology, *J. Geophys. Res.*, 109, C12003, 2004.
- Degens, E. T., Behrendt, M., Gotthard, B. and Reppmann, E.: Metabolic fractionation of carbon isotopes in marine plankton-II, Data on samples collected off the coasts of Peru and Ecuador. *Deep Sea Res.* 15, 11-20, 1968.
- DeMaster, D. J.: The supply and accumulation of silica in the marine environment, *Geochimica acta*, 45(10), 1715-1732, 1981.
- Devol, A. H.: Bacterial oxygen uptake kinetics as related to biological processes in oxygen deficient zones of the oceans, *Deep Sea Res.* 25, 137-146, 1978.
- Dewitte, B., Illig, S., Renault, L., Gourbanova, K., Takahashi, K. and Gushchina, D.: Modes of variability between sea surface temperature and wind stress intraseasonal anomalies along the coast of Peru from satellite observation, *J. Geophys. Res.* 116, 04028, doi:10.1029/2010JC006495, 2011.
- Dewitte, B., Vazquez-Cuervo, J., Gourbanova, K., Illig, S., Takahashi, K., Cambon, G., Purca, S., Correa, D., Gutierrez, D., Sifeddine, A. and Ortlieb, L.: Change in El Niño flavours over 1958-2008: Implications for the long-term trend of the upwelling off Peru, *Deep Sea Res II*, 77-80, 143-156, 2012.
- Diaz, J., Ingall, E., Benitez-Nelson, C., Paterson, D., de Jonge, M. D., McNulty, I. and Brandes, J. A.: Marine polyphosphate: a key player in geologic phosphorus sequestration, *Sciences*, 320, 652-655, 2008.
- Garcia-Robledo, E., Padilla, C. C., Aldunate, M., Stewart, F. J., Ulloa, O., Paulmier, A., Gregori, G. and Revsbech, N. P.: Cryptic Oxygen cycling in Anoxic Marine Zones, *Proc. Natl. Acad. Sci. U.S.A.*, 114(31), 8319-8324, doi:10.1073/pnas.1619844114, 2017.
- Heimbürger, L. E., Lavigne, E., Migon, C., D'ortenzio, F., Estournel, C., Coppola, L. and Miquel, J. C. Temporal variability of vertical flux at the DYFAMED time-series station (Northwestern Mediterranean Sea), *Prog. Oceanogr.*, 119, 59-67, 2013.
- Helmke, P., Romero, O. and Fischer, G.: Northwest African upwelling and its effect on offshore organic carbon export to the deep sea, *Global Biogeochem. Cycles*, 19, GB4015, 2005.



- Hirata, T., Hardman-Mountford, N. J., Brewin, R. J. W., Aiken, J., Barlow, R., Suzuki, K., Isada, T., Howell, T., Hashioka, T., Noguchi-Aita, M. and Yamanaka, Y.: Synoptic relationships between surface Chlorophyll-a and diagnostic pigments specific to phytoplankton functional types, *Biogeosciences*, 8(2), 311-327, 2011.
- Illig, S., Dewitte, B., Goubanova K., Cambon, G., Boucharel, J., Monetti, F., Romero, C., Purca, S. and Flores, R.: Forcing mechanisms of intraseasonal SST variability off central Peru in 2000–2008, *J. Geophys. Res. Oceans*, 119, 3548–3573, doi:[10.1002/2013JC009779](https://doi.org/10.1002/2013JC009779), 2014.
- Kalvelage, T., Lavik, G., Lam, P., Contreras, S., Arteaga, L., Löscher, C. R. and Kuypers, M. M.: Nitrogen cycling driven by organic matter export in the South Pacific oxygen minimum zone, *Nature geoscience*, 6(3), 228-234, 2013.
- Keil, R. G., Neibauer, J. A., Biladeau, C., van der Elst, K. and Devol, A. H.: A multiproxy approach to understanding the « enhanced » flux of organic matter through the oxygen-deficient waters of the Arabian Sea, *Biogeosciences*, 13, 2077-2092, 2016.
- Lam, P., Lavik, G., Jensen, M. M., Van de Vossenberg, J., Schmidt, M., Woebken, D., Gutierrez, D., Amann, M., Jetten, S. M. and Kuypers, M. M.: Revising the nitrogen cycle in the Peruvian oxygen minimum zone, *Proc. Natl. Acad. Sci. U.S.A.*, 106(12), 4752-4757, 2009.
- Lampitt, R. S., Noji, T. and Von Bodungen, B.: What happens to zooplankton faecal pellets? Implications for material flux, *Marine Biology*, 104.1, 15-23, 1990.
- Law, C. S., Brévière, E., De Leeuw, G., Garçon, V., Guieu, C., Kieber, D. J., Konradowitz, S., Paulmier, A., Quinn, P. K., Saltzman, E. S., Stefels, J. and von Glasow, R.: Evolving research directions in surface ocean–lower atmosphere (SOLAS) science, *Environ Chem.*, <http://dx.doi.org/10.1071/EN12159>, 2012.
- León, V., Paulmier, A., Ledesma, J., Croot, P., Graco, M., Flores, G., Morón, O. and Tenorio, J.: pH como un Trazador de la Variabilidad Biogeoquímica en el Sistema de Humboldt, *Boletín del IMARPE*, 26(1-2), 2011.
- Lewis, E. and Wallace, D. W. R.: Program Developed for CO₂ System Calculations, Edited by ORNL/CDIAC-105a., Carbon Dioxide Information Analysis Center, Oak Ridge National Laboratory, U.S. Department of Energy, Oak Ridge, Tennessee, 1998.
- Libes, S. M. and Deuser, W. G.: The isotope geochemistry of particulate nitrogen in the Peru upwelling area and the Gulf of Maine, *Deep Sea Research Part A, Oceanographic Research Papers*, 35(4), 517-533, 1988.
- Lipschultz, F., Wofsy, S.C., Ward, B. B., Codispoti, L. A., Friedrich, G., Elkins, J. W.: Bacterial transformations of inorganic nitrogen in the oxygen deficient waters of the Eastern Tropical South Pacific Ocean, *Deep Sea Res.*, 35(10), 1513-1541, 1990.
- Loucaides, S., Van Capellen, P. and Behrends, T: Dissolution of biogenic silica from land to ocean: Role of salinity and pH, *Limnol Oceanogr.*, 53(4), 1614-1621, 2008.



- Lueker, T. J., Dickson, A. G. and Keeling, C. D.: Ocean pCO₂ calculated from dissolved inorganic carbon, alkalinity, and equations for K₁ and K₂: validation based on laboratory measurements of CO₂ in gas and seawater at equilibrium, *Marine Chemistry*, 70(1–3), 105-119, 2000.
- Martin J. H., Knauer, G. A., Karl, D. M. and Broenkow, W. W.: VERTEX: carbon cycling in the NE Pacific, *Deep Sea Res.*, 34, 267-285, 1987.
- Marsay, C. M., Sanders, R. J., Henson, S. A., Pabortsava, K., Achterberg, E. P. and Lampitt, R. S.: Attenuation of sinking particulate organic carbon flux through the mesopelagic ocean, *Proc. Natl. Acad. Sci. U.S.A.*, 112(4), 1089-1094, 2015.
- Mayers, P. A.: Preservation of elemental and isotopic source identification of sedimentary organic matter, *Chem. Geol.*, 114, 239-302, 1993.
- 10 McDonnell, A. M. P., Boyd, P. W. and Buesseler, K. O.: Effects of sinking velocities and microbial respiration rates on the attenuation of particulate carbon fluxes through the mesopelagic zone, *Global Biogeochem. Cycles*, 29(2), 175-193, 2015.
- Miquel, J. C., Martin, J., Gasser, B., Rodriguez-y-Baena, A., Toubal, T. and Fowler, S. W.: Dynamics of particles flux and carbon export in the northwestern Mediterranean Sea: A two scale time-series study at the DYFAMED site, *Prog. Oceanogr.*, 91, 451-481, 2011.
- 15 Moffitt, S. E., Moffitt, R. A., Sauthoff, W., Davis, C. V., Hewett, K. and Hill, T. M.: Paleooceanographic Insights on Recent Oxygen Minimum Zone Expansion: Lessons for Modern Oceanography, *PLoS ONE*, 10(1): e0115246, 2015.
- Montes, I., Colas, F., Capet, X. and Schneider, W.: On the pathways of the equatorial subsurface currents in the eastern equatorial Pacific and their contribution to Peru-Chile Undercurrent, *J. Geophys. Res.*, 115, C09003, doi:10.1029/2009JC005710, 2010.
- 20 Ohkouchi, N., Ogawa, N. O., Chikaraishi, Y., Tanaka, H. and Wada, E.: Biochemical and physiology bases for the use of carbon and nitrogen isotopes in environmental and ecological studies, *Prog. Earth Planet. Sci.*, 2:1, doi: 10.1186/s40645-015-0032-y, 2015.
- Orr, J. C. et al.: Anthropogenic ocean acidification over the twenty-first century and its impact on calcifying organisms, *Nature*, 437, 681-686, doi:10.1038/nature04095, 2005.
- 25 Packard, T. T., Osma, N., Fernández-Urruzola, I., Codispoti, L. A., Christensen, J. P. and Gómez, M.: Peruvian upwelling plankton respiration: calculations of carbon flux, nutrient retention efficiency, and heterotrophic energy production, *Biogeosciences*, 12, 2641-2654, doi:10.5194/bg-12-2641-2015, 2015.
- Pantoja, S., Sepulveda, J. and Gonzalez, H. E.: Decomposition of sinking proteinaceous material during fall in the oxygen minimum zone off northern Chile, *Deep Sea Res. I.*, 51, 55-70, 2004.
- 30 Paulmier, A., Ruiz-Pino, D., Garçon, V. and Farias, L.: Maintaining of the Eastern South Pacific Oxygen Minimum Zone (OMZ) off Chile, *Geophys. Res. Lett.*, 33(20), L20601, 2006.



- Paulmier, A., Ruiz-Pino, D. and Garçon, V.: The oxygen minimum zones (OMZ) off Chile as intense source of CO₂ and N₂O, *Cont. Shelf Res.*, 28(20), 2746-2756, 2008.
- Paulmier, A., Kriest, I. and Oschlies, A.: Stoichiometries of remineralisation and denitrification in global biogeochemical ocean models, *Biogeosciences*, 6, 923–935, doi:10.5194/bg-6-923-2009, 2009.
- 5 Paulmier, A. and Ruiz-Pino, D.: Oxygen minimum zones (OMZs) in the modern ocean, *Prog. Oceanogr.*, 80(3-4), 113-128, 2009.
- Pennington, J. T., Mahoney, K. L., Kuwahara, V. S., Kolber, D. D., Calnics, R. and Chavez, F. P.: Primary production in the eastern tropical Pacific: A review, *Prog. Oceanogr.*, 66, 285-317, 2006.
- Ramaiah, N., Raghukumar, S. and Gauns, M.: Bacterial abundance and production in the central and eastern Arabian Sea, *Current Science*, 71(11), 878-882, 1996.
- 10 Redfield, A. C., Ketchum, B. H. and Richards, F. A., The influence of organism on the composition of the seawater, *The Sea*, 2, edited by M. N. Hill, pp 26-77, Interscience, New-York, 1963.
- Roullier, F., Berline, L., Guidi, L., Durrieu De Madron, X., Picheral, M., Sciandra, A., Pesant, S., and Stemmann, L.: Particle size distribution and estimated carbon flux across the Arabian Sea oxygen minimum zone, *Biogeosciences*, 11, 4541-4557, <https://doi.org/10.5194/bg-11-4541-2014>, 2014.
- 15 Siegel, D. A., Granata, T. C., Michaelis, A. F. and Dickey, T. D.: Mesoscale eddy diffusion, particle sinking and the interpretation of sediment trap data, *J. Geophys. Res.*, 95(C4), 5305-5311, 1990.
- Sobarzo, M., Bravo, L., Donoso, D., Garcès-Vargas, J. and Schneider, W.: Coastal upwelling and seasonal cycles that influence the water column over the continental shelf of central Chile, *Prog. Oceanogr.*, 75, 363-382, 2007.
- 20 Stemmann, L., Jackson, G. A. and Ianson, D.: A vertical model of particle size distributions and fluxes in the midwater column that includes biological and physical processes-Part I: model formulation, *Deep Sea Res. Part. I.*, 51, 865-884, 2004.
- Stemmann, L. and Boss, E.: Plankton and particle size and packaging: from determining optical properties to driving the biological pump, *Annu. Rev. Mar. Sci.*, 4, 263–290, 2012.
- Stewart, F. J., Ulloa, O. and DeLong, E. F.: Microbial metatranscriptomics in a permanent marine oxygen minimum zone, *Environ. Microbiol.*, 14(1), 23-40, 2012.
- 25 Strickland, J. D. H. and Parsons, T. R.: A practical handbook of sea water analysis, The fisheries research board of Canada, Bulletin N°25, 1972.
- Suess, E.: Particulate organic carbon flux in the ocean-surface productivity and oxygen utilization, *Nature*, 288, 206-263, 1980.
- Sun, M-Y., Aller, R. C., Lee C. and Wakeham, G.: Effect of oxygen and redox oscillation on degradation of cell-associated lipids in superficial marine sediments, *Geochemica and Cosmochimica Acta*, 66(11), 2003-2012, 2002.
- 30



Van Mooy, B. A. S., Keil, R. G. and Devol, A. H.: Impact of suboxia on sinking particulate organic carbon: enhanced carbon flux and preferential degradation of amino-acids via denitrification, *Geochimica and Cosmochimica Acta*, 66(3), 457-465, 2002.

5 Waniek, J., Koeve, W., Prien, D.: Trajectories of sinking particles and the catchment areas above sediment traps in the northeast Atlantic, *J. Mar. Res.*, 58, 983-1006, 2000.



Tables captions

Table 1: POC flux, transfer efficiency T_{eff} and b for each main T_{eff} range. T_{eff} is determined from $\%Flux_{149m}/Flux_{34m}$ (Eq. 1). b is the coefficient from the Martin's curves theory (Suess, 1980; Martin et al., 1987). *Italic and non-italic values correspond to the fluxes at 34 m and 149 m, respectively. On the last lines of the table, bold colored values in red, yellow and blue correspond to POC fluxes, T_{eff} and b averaged values for low, intermediate and high T_{eff} ranges, respectively, with the relative standard deviation between samples ($\pm SD\%$). Analysis accuracy on the POC fluxes is $\pm 0.2\%$, inducing an absolute uncertainty on its vertical transfer efficiency estimated from a logarithmic expansion of $\pm 0.2\%$ (cf. Methods).*

Table 2: Oxygen concentration in the upper and bottom OMZ layer, proportion of Polychaetes number of individuals, and POC flux/ O_2 concentration ratios. O_2 concentration corresponds to the oxygen concentration averaged on the sampling acquisition periods: $[\overline{O_2}]_{7days,15min}$ for AMOP1 and $[\overline{O_2}]_{11days,15min}$ for AMOP2. %Poly corresponds to the percentage of number of individuals of Polychaetes relatively to all collected swimmers, per day. The POC flux / O_2 concentration corresponds to the ratio of both weekly quantities (POC flux collected in the trap and $[\overline{O_2}]_{1week,15min}$ determined from the O_2 sensor). *Italic values correspond to the $[O_2]$, %Poly and POC flux / O_2 concentration at the upper trap, and non-italic values at the lower trap. On the last lines of the table, bold colored values in red, yellow and blue correspond to $[O_2]$, %Poly and POC flux / $[O_2]$ averaged values for low, intermediate and high T_{eff} ranges, respectively, with the relative standard deviation between samples ($\pm SD\%$). %Poly is determined from a significant number of Polychaetes individuals collected per sample (4607 in average, between 50 and 31099). Note that Polychaetes and copepods represent 97% of all the reported swimmers.*

Table 3: Organic elemental fluxes and the corresponding molar ratios as well as inorganic and isotopic fluxes, and their transfer efficiencies for each main T_{eff} range.

a) Organic Elementary fluxes in $mg.m^{-2}.d^{-1}$ and their transfer efficiency in % (T_{eff} , T_{effPON} , T_{effPOP} , T_{effBSi} ; cf. Table 1 caption for calculation) in terms of Particulate Organic Carbon (POC), Nitrogen (PON), Phosphorus (POP) and biogenic Silica (BSi) for each three main T_{eff} ranges (low in red, intermediate in yellow, high in blue) with the temporal standard deviation between samples ($\pm SD\%$). *Italic and non-italic values correspond to the fluxes at 34 m and 149 m, respectively. Analysis accuracies on the elementary fluxes are $\pm 0.2\%$ for both POC and PON, $\pm 3\%$ for POP, and $\pm 5\%$ for BSi, inducing an absolute uncertainty of $\pm 0.2\%$ (T_{eff}), $\pm 0.2\%$ (T_{effPON}), $\pm 3\%$ (T_{effPOP}) and $\pm 5\%$ (T_{effBSi}) on the transfer efficiency (cf. Methods).*

b) Values of elementary ratios (C:N, C:P, N:P, and Si:C, Si:N, Si:P) and transfer efficiency of these ratios in % ($T_{effC:N}$, $T_{effC:P}$, $T_{effN:P}$, and $T_{effSi:N}$, $T_{effSi:N}$, $T_{effSi:P}$; cf. Table 1 caption for calculation) for each three main T_{eff} ranges (low in red, intermediate in yellow, high in blue) with the temporal standard deviation between samples ($\pm SD\%$). *Italic and non-italic values correspond to the fluxes at 34 m and 149 m, respectively. Analysis accuracies on the elementary ratios are ± 0.4 , 3.2, 3.2% and ± 5.2 , 5.2, 8% for C:N, C:P and N:P and for Si:C, Si:N and Si:P, respectively, inducing an absolute uncertainty of $\pm 0.9\%$ ($T_{effC:N}$), $\pm 6.3\%$ ($T_{effC:P}$), $\pm 6\%$ ($T_{effN:P}$), and of $\pm 12\%$ ($T_{effSi:C}$), $\pm 13.4\%$ ($T_{effSi:N}$) and $\pm 19\%$ ($T_{effSi:P}$) on the transfer efficiency (cf. Methods). Classical (reference) molar ratios have been reported on the second lines from Redfield et al. (1963) and Brezinski (1985).*

c) Fluxes of inorganic calcium carbonate ($CaCO_3$) in $mgCa.m^{-2}.d^{-1}$ and of carbon isotopic ratio ($\delta^{13}C$) and nitrogen isotopic ratio ($\delta^{15}N$) in ‰ and their transfer efficiency in % ($T_{effCaCO_3}$, T_{eff13C} , T_{eff15N} ; cf. Table 1 caption for calculation) for each three main T_{eff} ranges (low in red, intermediate in yellow, high in blue) with the temporal standard deviation between samples ($\pm SD\%$). *Italic and non-italic values correspond to the fluxes at 34 m and 149 m, respectively. Analysis accuracies on the elementary fluxes are $\pm 3\%$ for $CaCO_3$, $\pm 0.006\%$ for $\delta^{13}C$ and $\pm 0.007\%$ for $\delta^{15}N$, inducing an absolute uncertainty of $\pm 3\%$ ($T_{effCaCO_3}$), $\pm 0.06\%$ (T_{eff13C}) and $\pm 0.26\%$ (T_{eff15N}) on the transfer efficiency (cf. Methods).*



| Sample name | Date in 2013 | | POC Fluxes | | Teff % | Error bar on Teff % | b |
|--------------------------|--------------|-------|--|---------------------|---------------------|------------------------------|-----------------------|
| | Start | End | 34 m mgC.m ⁻² .d ⁻¹ | 149 m | | | |
| AMOP1-S1 | 06/01 | 13/01 | 139.40 | 98.63 | 71 | ± 1 | 0.23 |
| AMOP1-S2 | 13/01 | 20/01 | 127.87 | 70.68 | 55 | ± 1 | 0.40 |
| AMOP1-S3 | 20/01 | 27/01 | 149.48 | 85.89 | 57 | ± 1 | 0.37 |
| AMOP1-S4 | 27/01 | 03/02 | 92.16 | 22.14 | 24 | ± 1 | 0.97 |
| AMOP1-S5 | 03/02 | 10/02 | 107.43 | 45.49 | 42 | ± 1 | 0.58 |
| AMOP1-S6 | 10/02 | 17/02 | 132.72 | 41.49 | 31 | ± 1 | 0.79 |
| AMOP1-S7 | 17/02 | 24/02 | 41.16 | 17.98 | 44 | ± 2 | 0.56 |
| AMOP1-S8 | 24/02 | 03/03 | 86.33 | 20.44 | 24 | ± 1 | 0.98 |
| AMOP1-S9 | 03/03 | 10/03 | 109.69 | 37.92 | 35 | ± 1 | 0.72 |
| AMOP1-S10 | 10/03 | 17/03 | 51.31 | 19.25 | 38 | ± 3 | 0.66 |
| AMOP1-S11 | 17/03 | 24/03 | 20.30 | 11.63 | 57 | ± 8 | 0.38 |
| AMOP1-S12 | 24/03 | 31/03 | 54.08 | 20.14 | 37 | ± 2 | 0.67 |
| AMOP2-S1 | 28/06 | 09/07 | 41.19 | 55.49 | 135 | ± 2 | -0.20 |
| AMOP2-S2 | 09/07 | 20/07 | 37.05 | 21.15 | 57 | ± 1 | 0.38 |
| AMOP2-S3 | 20/07 | 31/07 | 17.15 | 18.18 | 106 | ± 5 | -0.04 |
| AMOP2-S4 | 31/07 | 11/08 | 19.42 | 6.21 | 32 | ± 4 | 0.77 |
| AMOP2-S5 | 11/08 | 22/08 | 17.91 | 12.22 | 68 | ± 4 | 0.26 |
| AMOP2-S6 | 22/08 | 02/09 | 6.45 | 9.59 | 149 | ± 12 | -0.27 |
| AMOP2-S7 | 02/09 | 13/09 | 470.49 | 8.28 | 2 | ± 0.1 | 2.73 |
| AMOP2-S8 | 13/09 | 24/09 | 395.10 | 4.93 | 1 | ± 0.1 | 2.97 |
| AMOP2-S9 | 24/09 | 05/10 | 172.94 | 7.20 | 4 | ± 0.3 | 2.15 |
| AMOP2-S10 | 05/10 | 16/10 | 135.00 | 6.97 | 5 | ± 0.3 | 2.01 |
| AMOP2-S11 | 16/10 | 27/10 | 180.91 | 4.78 | 3 | ± 0.2 | 2.46 |
| AMOP2-S12 | 27/10 | 07/11 | 83.04 | 3.00 | 4 | ± 1 | 2.25 |
| High Teff | | | 71 (±89%) | 40 (±88%) | 59 (±9%) | | 0.36 (±16%) |
| Intermediate Teff | | | 77 (±49%) | 26 (±50%) | 34 (±21%) | | 0.74 (±20%) |
| Low Teff | | | 240 (±65%) | 6 (±33%) | 3 (±48%) | | 2.43 (±15%) |

Table 1



| Sample name | Date in 2013 | | [O ₂] | | %Poly | POC/[O ₂] |
|-------------|--------------|--------------------------|-----------------------|------------|------------|-----------------------|
| | Start | End | μmol.kg ⁻¹ | | %/day | |
| | | | 34 m | 147 m | 34 m | 34 m |
| AMOP1-S1 | 06/01 | 13/01 | 6.74 | 3.09 | 12.4 | 20.7 |
| AMOP1-S2 | 13/01 | 20/01 | 3.48 | 3.08 | 13.2 | 36.7 |
| AMOP1-S3 | 20/01 | 27/01 | 4.91 | 3.07 | 11.7 | 30.4 |
| AMOP1-S4 | 27/01 | 03/02 | 6.23 | 3.06 | 9.7 | 14.8 |
| AMOP1-S5 | 03/02 | 10/02 | 4.5 | 3.07 | 13.6 | 23.9 |
| AMOP1-S6 | 10/02 | 17/02 | 5.49 | 3.07 | 8.9 | 24.2 |
| AMOP1-S7 | 17/02 | 24/02 | 3.73 | 3.06 | 3.8 | 11.0 |
| AMOP1-S8 | 24/02 | 03/03 | 12.52 | 3.07 | 6.3 | 6.9 |
| AMOP1-S9 | 03/03 | 10/03 | 9.37 | 3.07 | 1.0 | 11.7 |
| AMOP1-S10 | 10/03 | 17/03 | 6.03 | 3.02 | 11.4 | 8.5 |
| AMOP1-S11 | 17/03 | 24/03 | 4.33 | 3.01 | 14.1 | 4.7 |
| AMOP1-S12 | 24/03 | 31/03 | 3.86 | 3.02 | 13.8 | 14.0 |
| | | | | | | |
| AMOP2-S1 | 28/06 | 09/07 | 34.1 | 3.62 | 0.7 | 1.21 |
| AMOP2-S2 | 09/07 | 20/07 | 41.35 | 3.56 | 1.1 | 0.9 |
| AMOP2-S3 | 20/07 | 31/07 | 56.69 | 4.05 | 0.8 | 0.3 |
| AMOP2-S4 | 31/07 | 11/08 | 66.22 | 4.85 | 0.1 | 0.3 |
| AMOP2-S5 | 11/08 | 22/08 | 115.7 | 11.84 | 0.0 | 0.2 |
| AMOP2-S6 | 22/08 | 02/09 | 69.35 | 5.76 | 0.1 | 0.1 |
| AMOP2-S7 | 02/09 | 13/09 | 89.06 | 6.33 | 0.3 | 5.3 |
| AMOP2-S8 | 13/09 | 24/09 | 31.61 | 4.65 | 0.4 | 12.5 |
| AMOP2-S9 | 24/09 | 05/10 | 38.2 | 4.85 | 0.6 | 4.5 |
| AMOP2-S10 | 05/10 | 16/10 | 68.63 | 4.43 | 0.3 | 2.0 |
| AMOP2-S11 | 16/10 | 27/10 | 100.15 | 3.59 | 0.4 | 1.8 |
| AMOP2-S12 | 27/10 | 07/11 | 34.22 | 3.08 | 0.6 | 2.4 |
| | | | | | | |
| | | | 34.0 | 4.9 | 8.0 | 14.6 |
| | | | (±143%) | (±79%) | (±86%) | (±121%) |
| | | High Teff | | | | |
| | | | 13.1 | 3.2 | 7.6 | 12.8 |
| | | | (±154%) | (±18%) | (±67%) | (±60%) |
| | | Intermediate Teff | | | | |
| | | | 60.3 | 4.5 | 0.4 | 4.7 |
| | | | (±50%) | (±25%) | (±35%) | (±85%) |
| | | Low Teff | | | | |

Table 2



| a) | PON | | T_{effPON} | POP | | T_{effPOP} | BSi | | T_{effBSi} |
|--------------------------|--|--------|---------------------|--|--------|---------------------|---|--------|---------------------|
| | $\text{mgN}\cdot\text{m}^{-2}\cdot\text{d}^{-1}$ | | | $\text{mgP}\cdot\text{m}^{-2}\cdot\text{d}^{-1}$ | | | $\text{mgSi}\cdot\text{m}^{-2}\cdot\text{d}^{-1}$ | | |
| | 34 m | 149 m | % | 34 m | 149 m | % | 34 m | 149 m | % |
| High Teff | 10.56 | 5.66 | 54 | 3.29 | 1.41 | 60 | 75.36 | 53.34 | 72 |
| | (±85%) | (±87%) | (±89%) | (±91%) | (±63%) | (±53%) | (±78%) | (±72%) | (±32%) |
| Intermediate Teff | 10.72 | 3.66 | 34 | 3.71 | 1.21 | 34 | 69.03 | 26.15 | 37 |
| | (±46%) | (±56%) | (±27%) | (±33%) | (±50%) | (±47%) | (±54%) | (±58%) | (±25%) |
| Low Teff | 41.23 | 0.91 | 2 | 4.93 | 0.53 | 14 | 495.00 | 9.47 | 3 |
| | (±61%) | (±18%) | (±47%) | (±64%) | (±98%) | (±81%) | (±105%) | (±81%) | (±119%) |

| b) | C:N | | $T_{\text{effC:N}}$ | C:P | | $T_{\text{effC:P}}$ | N:P | | $T_{\text{effN:P}}$ |
|--------------------------|--------|--------|---------------------|--------|--------|---------------------|--------|--------|---------------------|
| | 6.63 | | | 106 | | | 16 | | |
| | 34 m | 149 m | % | 34 m | 149 m | % | 34 m | 149 m | % |
| High Teff | 7.59 | 8.26 | 111 | 60.72 | 68.01 | 117 | 8.3 | 8.26 | 112 |
| | (±13%) | (±6%) | (±16%) | (±31%) | (±39%) | (±41%) | (±44%) | (±37%) | (±49%) |
| Intermediate Teff | 8.27 | 8.36 | 102 | 53.78 | 54.93 | 121 | 6.4 | 6.64 | 117 |
| | (±14%) | (±14%) | (±16%) | (±38%) | (±32%) | (±54%) | (±36%) | (±32%) | (±46%) |
| Low Teff | 6.67 | 7.38 | 110 | 128.53 | 49.02 | 38 | 19.15 | 6.61 | 35 |
| | (±11%) | (±22%) | (±16%) | (±22%) | (±66%) | (±68%) | (±15%) | (±62%) | (±67%) |

| | Si:C | | $T_{\text{effSi:C}}$ | Si:N | | $T_{\text{effSi:N}}$ | Si:P | | $T_{\text{effSi:P}}$ |
|--------------------------|--------|--------|----------------------|--------|--------|----------------------|--------|--------|----------------------|
| | 0.14 | | | 0.94 | | | 15 | | |
| | 34 m | 149 m | % | 34 m | 149 m | % | 34 m | 149 m | % |
| High Teff | 0.50 | 0.63 | 121 | 3.71 | 5.37 | 137 | 31.45 | 39.00 | 138 |
| | (±52%) | (±57%) | (±24%) | (±46%) | (±59%) | (±37%) | (±60%) | (±45%) | (±44%) |
| Intermediate Teff | 0.40 | 0.44 | 110 | 3.36 | 3.79 | 113 | 22.04 | 24.63 | 131 |
| | (±50%) | (±54%) | (±10%) | (±54%) | (±65%) | (±18%) | (±60%) | (±58%) | (±47%) |
| Low Teff | 0.71 | 0.61 | 95 | 4.86 | 5.01 | 112 | 93.42 | 28.87 | 27 |
| | (±56%) | (±67%) | (±79%) | (±51%) | (±83%) | (±96%) | (±51%) | (±69%) | (±51%) |

| c) | $\delta^{13}\text{C}$ | | $T_{\text{eff}^{13}\text{C}}$ | $\delta^{15}\text{N}$ | | $T_{\text{eff}^{15}\text{N}}$ | CaCO_3 | | T_{effCaCO_3} |
|--------------------------|-----------------------|--------|-------------------------------|-----------------------|--------|-------------------------------|---|--------|------------------------|
| | ‰ | | | ‰ | | | $\text{mgCa}\cdot\text{m}^{-2}\cdot\text{d}^{-1}$ | | |
| | 34 m | 149 m | % | 34 m | 149 m | % | 34 m | 149 m | % |
| High Teff | -21.24 | -19.85 | 93 | 6.71 | 7.54 | 113 | 10.21 | 6.9 | 127 |
| | (±5%) | (±6%) | (±4%) | (±13%) | (±23%) | (±23%) | (±132%) | (±79%) | (±70%) |
| Intermediate Teff | -21.18 | -19.93 | 94 | 6.4 | 9.04 | 156 | 14.52 | 3.62 | 30 |
| | (±3%) | (±3%) | (±2%) | (±31%) | (±19%) | (±40%) | (±50%) | (±52%) | (±65%) |
| Low Teff | -19.47 | -18.86 | 97 | 7.42 | 7.68 | 107 | 107.21 | 1.76 | 7 |
| | (±3%) | (±8%) | (±6%) | (±20%) | (±9%) | (±22%) | (±131%) | (±88%) | (±170%) |

Table 3



Figures captions

Figure 1: Study area, OMZ O₂ conditions and design of the mooring.

- a) Map of the Eastern South Pacific Oxygen Minimum Zone (in red with $[O_2]_{\text{minimal}} < 20 \mu\text{mol.kg}^{-1}$ from WOA2013 climatology). This map includes the location of the AMOP mooring (white cross, 77.40°W - 12.02°S) off Peru.
- b) Vertical distribution of the oxygen concentration at the mooring location (from WOA2013 climatology with the two sediment traps location in black square).
- c) Design of the fixed mooring line including two sediment traps, PPS3 with two inclinometers at 34 m near the oxycline and at 149 m in the OMZ core, as well as 5 PTS-O₂ (SBE37-ODO63) at 34, 76, 147 and 160 m, a fluorometer at 31 m, and complementary temperature sensors (SBE56). Sensor depths are indicated to ± 1 m, estimated from sensor pressure and inclinometer data (cf. Methods).

Figure 2: Time series in 2013 for POC flux (left handed scale) at 34 m (black bar) and 149 m (white bar) **and the corresponding transfer efficiency** (T_{eff} , from Eq.1, gray line, right-handed scale), covering AMOP1 (a) and AMOP2 (b) periods. Error bars correspond to the accuracy of analytical determination for the POC flux and is estimated through a logarithmic expansion of Eq. 1 for T_{eff} . (cf. Methods, Tab. 3a and Tab. S1 for details).

Figure 3: Time series in 2013 of the oxygen concentration ($\mu\text{mol.kg}^{-1}$) covering AMOP1 and AMOP2 periods, acquired on the mooring location line through oxygen sensors at 34, 76, 147 and 160 m depth with a 15 min acquisition frequency and vertically interpolated (cf. Fig. 1c and Methods). The dashed horizontal white lines indicate the depth of the traps.

Figure 4: Time series documented at the mooring site in 2013 of oxygen concentration and density at the upper trap, of Mixed Layer Depth (MLD) and wind speed in surface, and of POC flux and fluorescence at the upper trap, for each sample. Left and right panels are for AMOP1 and AMOP2, respectively.

- a-b) Daily oxygen concentration ($[\overline{O_2}]_{1\text{day},15\text{min}}$, blue line, and density (red line) calculated from pressure, temperature and salinity data acquired with the PTS sensors (cf. Fig. 1c), at 34 m depth.
- c-d) Daily mixed layer depth (purple) and wind velocity (grey) from ASCAT satellite.
- e-f) Weekly POC flux at 34 m (black) in $\text{mgC.m}^{-2}.\text{d}^{-1}$ and daily fluorescence data at 31 m (green) in relative unit.
- For more details, cf. Methods.

Figure 5: Vertical transfer efficiency for POC (T_{eff}) versus POC flux at the upper trap.

T_{eff} versus POC flux in $\text{mgC.m}^{-2}.\text{d}^{-1}$ at 34 m for AMOP2 dataset filtering samples with $T_{\text{eff}} > 100\%$ (thus excluding AMOP2-S1, -S3 and -S6, cf. Section “Significance of the transfer efficiency”), with power tendency line ($R^2 = 0.88$).

Figure 6: Average mass flux and particles composition at the upper sediment trap (34m) averaged by main T_{eff} ranges.

- a) Histograms of POC fluxes in $\text{mgC.m}^{-2}.\text{d}^{-1}$ (cf. Fig. 2) with error bars corresponding to the standard deviation.
- b) Sector diagrams of particles composition (mol%) in terms of Particulate Organic Carbon (POC), Particulate Organic Nitrogen (PON), Particulate Organic Phosphorus (POP) and Biogenic Silica (BSi). The values indicated in % correspond to the abundance of one element relative to the sum of the four other elements analyzed here for the OM. For more details, cf. Tables S1 and S2.

Note that due to its specific OM quality at 34 m, AMOP2-S4 sample has been extracted from the intermediate T_{eff} range and represented separately.

Figure 7: Mean transfer efficiency for the main components of the particles fluxes (related to POC, PON, POP, BSi, CaCO₃, and to particulate $\delta^{13}\text{C}$ and $\delta^{15}\text{N}$), **as a function of the three main T_{eff} ranges** defined from POC fluxes. The transfer efficiencies for PON (T_{effPON}), POP (T_{effPOP}), bSi (T_{effBSi}), CaCO₃ (T_{effCaCO_3}), $\delta^{13}\text{C}$ ($T_{\text{eff}^{13}\text{C}}$) and $\delta^{15}\text{N}$ ($T_{\text{eff}^{15}\text{N}}$) are derived from Eq.1, as for T_{eff} . Error bars represent the associated Standard Deviation of the elemental transfer for the considered T_{eff} ranges (More details in Tab. 3).

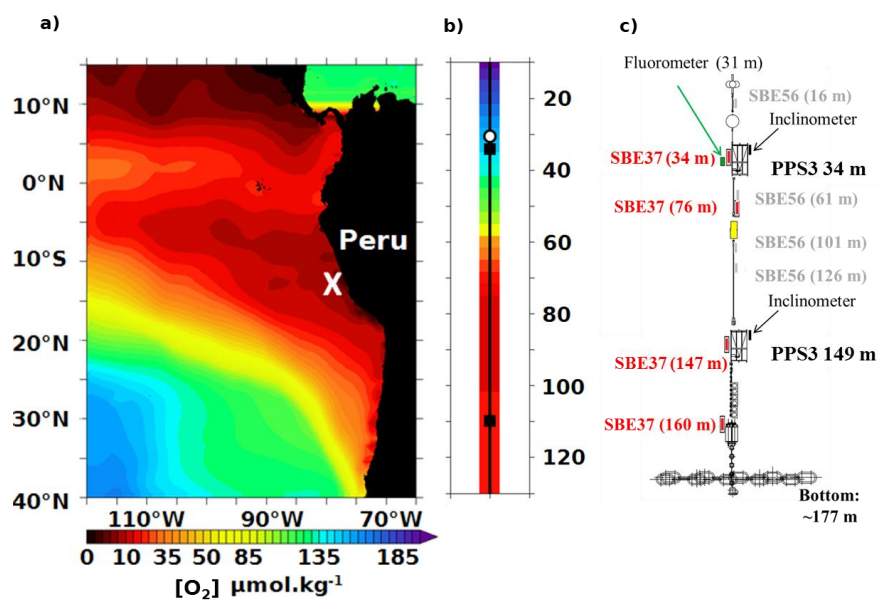


Figure 1

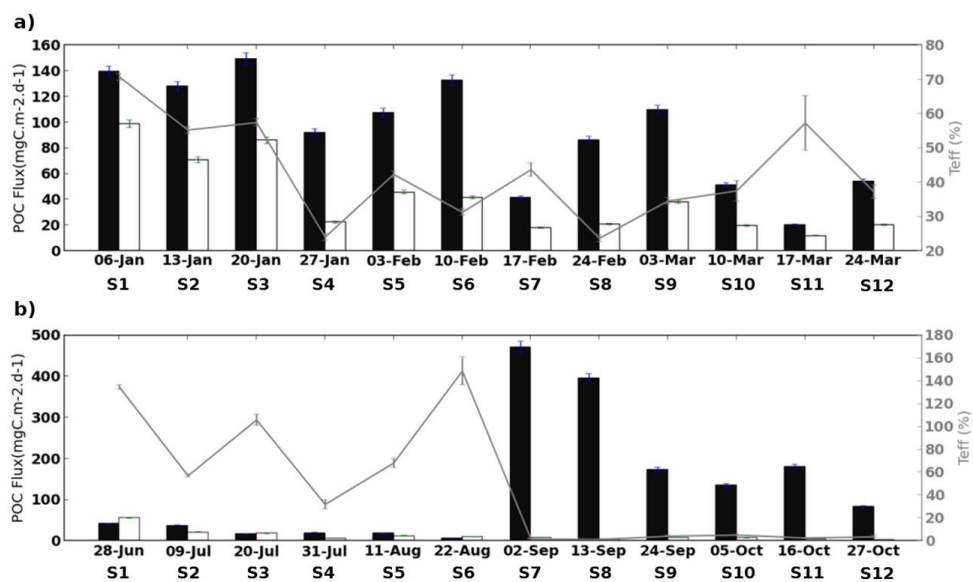


Figure 2

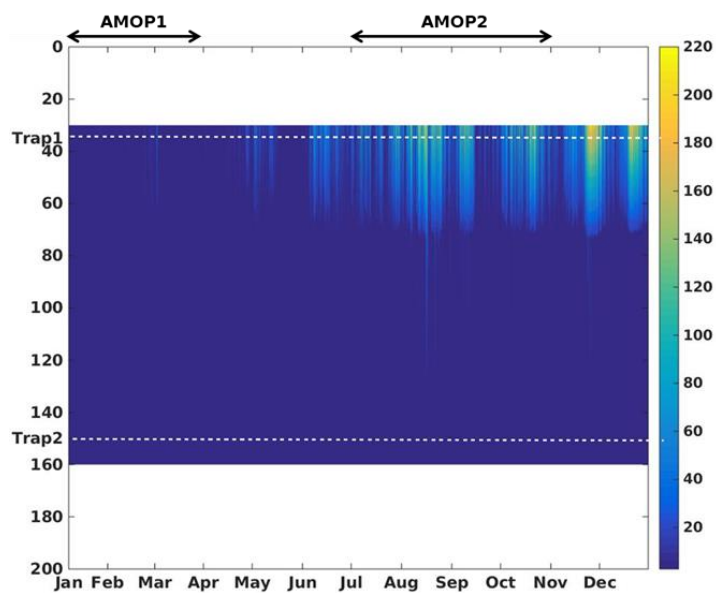


Figure 3

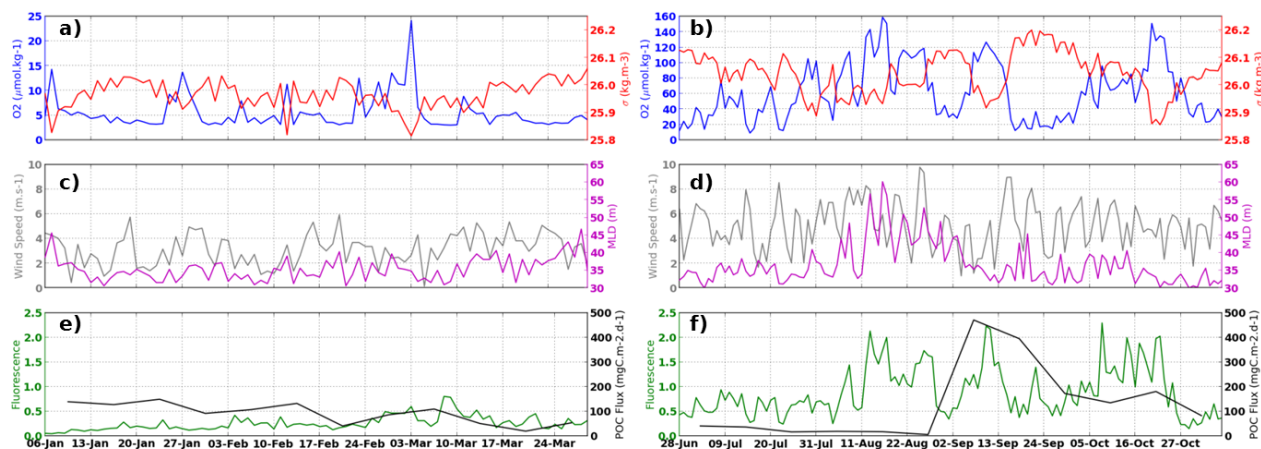


Figure 4

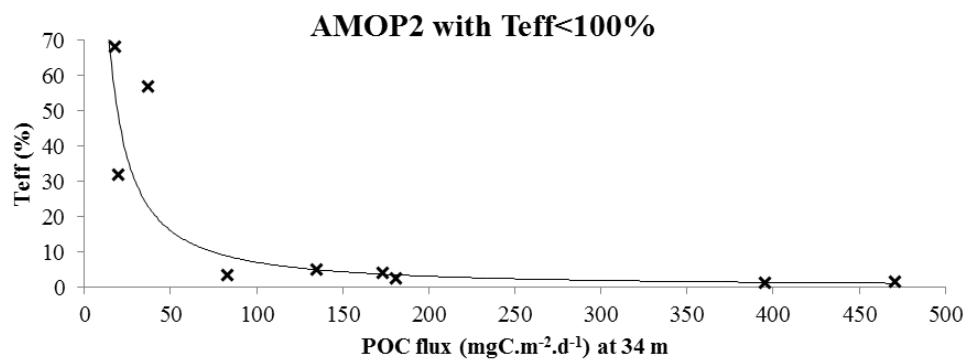


Figure 5

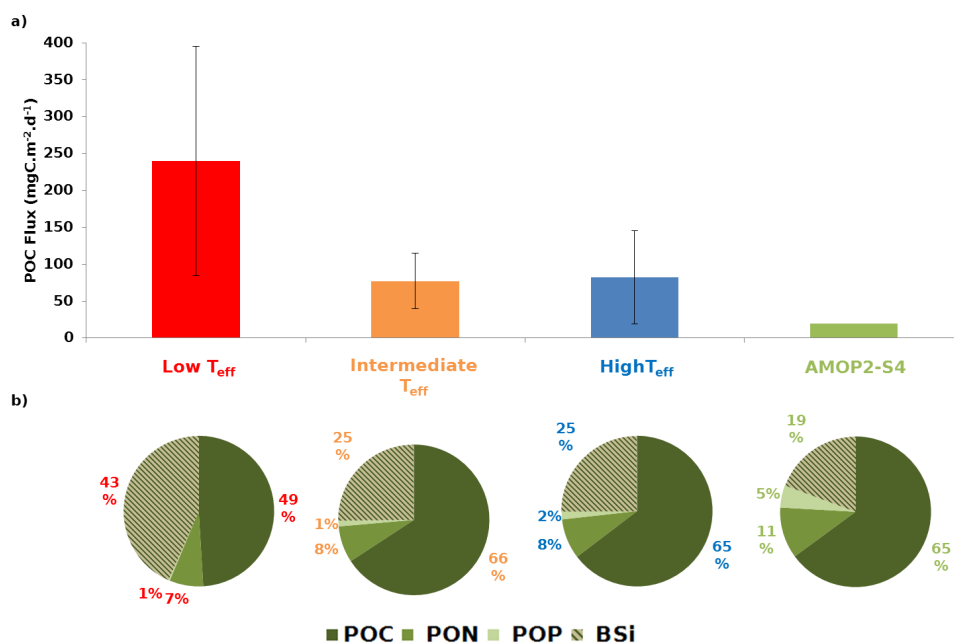


Figure 6

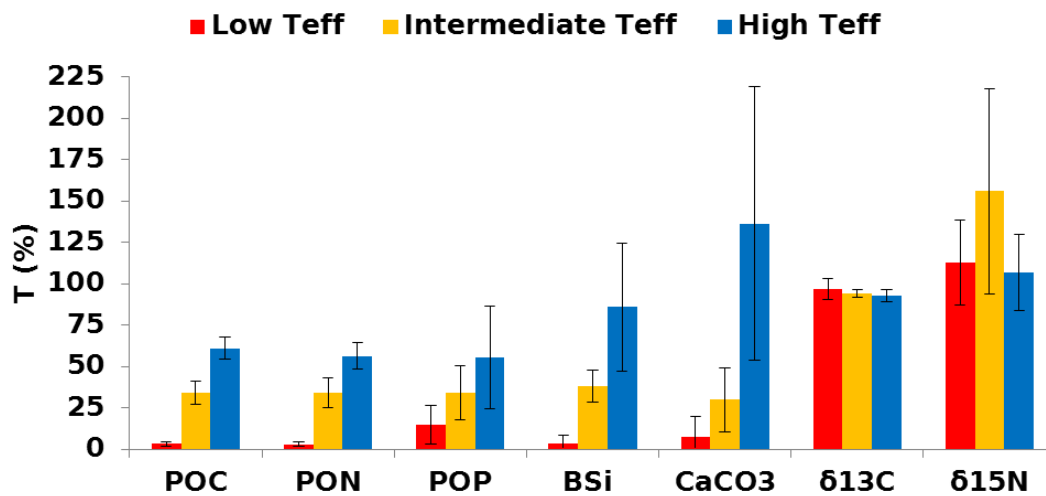


Figure 7